have suggested that this result is due to a genetic susceptibility associated with deregulated immune responses and an increased viral or proviral load (Nagai et al., 1998).

Mesenchymal stromal cells (MSCs) are multipotent precursor cells with numerous immunomodulatory properties that have been isolated from multiple tissues, such as the bone marrow (BM), adipose tissue, umbilical cord blood, dental pulp, and the connective tissue of almost all organs (Friedenstein et al., 1976; da Silva Meirelles et al., 2006). The minimum criteria for MSC definition include plastic adherence, the surface expression of CD105 (endoglin, SH2), CD73 (ecto-5′-nucleotidase), and CD90 (Thy1), the absence of hematopoietic markers, such as CD45, CD34, CD14, CD11b, CD79α, CD19, and HLA-DR, and their *in vitro* differentiation into chondrogenic, adipogenic, and osteogenic cells (Dominici et al., 2006). These stromal cells have remarkable immunomodulatory and regenerative properties due to the secretion of anti-inflammatory proteins and suppress the activity of various immune cells, such as alloantigen-activated T and B lymphocytes. In contrast, it has been reported that the functionality and ability of MSCs to inhibit immune cells can be modulated by inflammatory mediators released from activated immune cells, such as IFN-γ, IL1β, and TNF-α. MSCs may provide a balance of immune responses by acquiring a pro-inflammatory or an anti-inflammatory capacity depending on the stimulus and the physiological conditions of the organism (Waterman et al., 2010; Auletta et al., 2012).

Due to the biological importance of MSCs, studies have investigated the interaction between MSCs and viruses and have demonstrated that MSCs can be cell targets for several infections (Marandin et al., 1995; Scadden et al., 1990; Smirnov et al., 2007; Choudhary et al., 2011). For example, human immunodeficiency virus (HIV-1) is able to infect bone marrow-derived MSCs, and this infection affects MSC biology, impairing their clonogenic potential, cell differentiation, and phenotype (Wang et al., 2002; Cotter et al., 2008, 2011, 2007). Human vessel wall-derived MSCs are also susceptible to HIV, and this susceptibility is connected with a dysregulation of their survival and differentiation potential (Gibellini et al., 2011). Human cytomegalovirus (CMV) infects MSCs, thereby changing their structure and function, and this process alters their morphological character and impairs their process of differentiation. Therefore, MSCs may be considered a site of CMV latency and reactivation (Smirnov et al., 2007; Wei et al., 2011). Other studies have shown that MSCs are susceptible to herpes simplex virus type-1 (HSV-1) and that this infection induces a cytopathic effect with viral productive replication (Choudhary et al., 2011).

Although MSC are considered a target of several viral infections, there are no reports in the literature on the susceptibility of MSCs to HTLV infection, and the biological effects of HTLV-1 on MSCs are unknown. Therefore, in this study, we demonstrate that HTLV-1 is able to infect human bone-marrow MSCs *in vitro* and induce alterations to the MSC phenotype. The interaction between HTLV-1 and MSC contributes to the current understanding of HTLV-1 dissemination and persistence and provides new information on HTLV-1 tropism and associated diseases.

Results

HTLV-1 exposition modifies MSC morphology

Morphology and ultrastructural analyses were performed to identify alterations in MSCs induced by HTLV-1. For this purpose, three distinct culture conditions were evaluated: (1) MSCs in the presence of 100 ng of cell-free virus, (2) MSCs co-cultured with MT2 cells in a transwell system, and (3) MSCs co-cultured with MT2 cells subjected to irradiation (60,000 Gy). As the control culture, MSCs were grown in the same medium in the absence of virus. The light microscope analyses showed that the MSC morphology was not affected by exposure to HTLV-1. The cells maintained their fibroblastoid-like, spindle-shaped morphology, similar to the control MSCs (Fig. 1A and B). However, the ultrastructural analysis of MSCs cultured in the presence of HTLV-1 showed morphological changes, including an increase in the number of intracellular vesicle structures, compared with the control MSC (Fig. 1C and D). In addition,

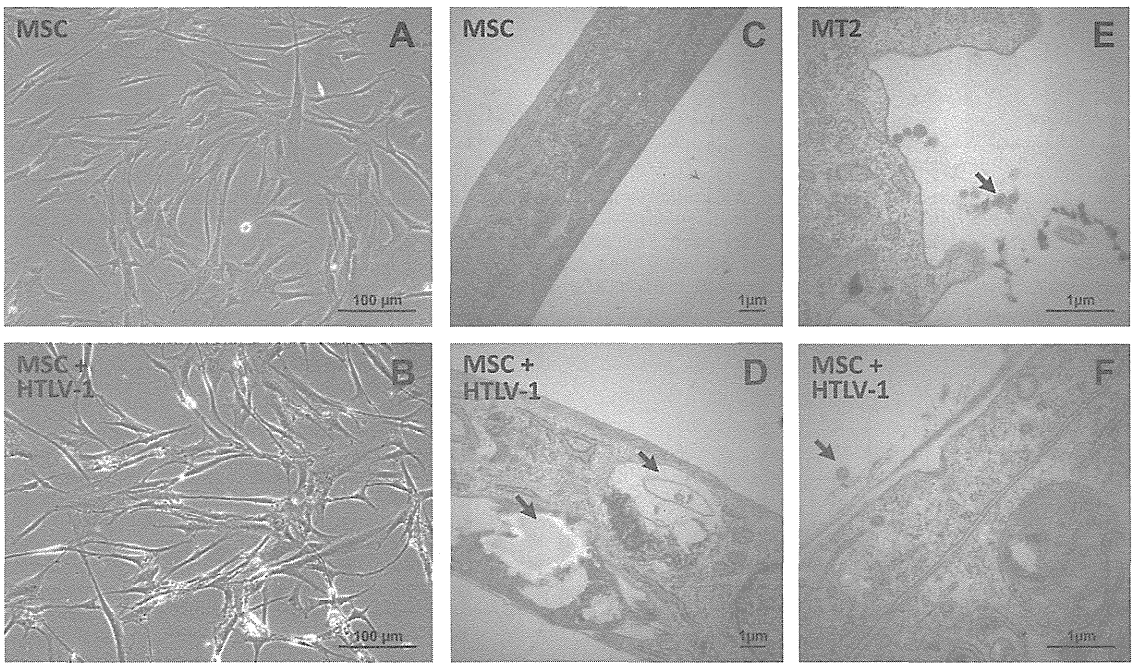

Fig. 1. Characterization of MSCs exposed to HTLV-1. (A and B) Morphological analysis by light microscopy of (A) control bone marrow (BM)-mesenchymal stromal cells (MSCs) and (B) MSCs exposed to HTLV. The scale bars represent 100 μm. (C–F) Ultrastructural analysis by transmission electron microscopy of (C) control MSCs and (D) MSCs exposed to HTLV with numerous intracellular vesicles (indicated by arrows); (E) HTLV-1 particles from MT2 cells are observed in the extracellular space (arrows), and (F) HTLV-1 virus particles are found in close association with MSCs (arrows). Scale bars = 1 μm.

we observed the release of HTLV-1 virions by MT2 cells (Fig. 1E) co-cultured in close proximity to MSCs (Fig. 1F).

MSCs exposed to HTLV-1 showed alterations in the immunophenotypic properties

To investigate the effect of HTLV-1 exposure on the physiological features of MSCs, we analyzed the expression level of MSC surface molecules by flow cytometry. The analysis revealed that the expression of adhesion molecules, such as VCAM-1 (CD106) and ICAM-1 (CD54), were significantly increased in MSCs exposed to HTLV-1 ($p < 0.01$) compared with the controls. The higher expression levels of CD106 and CD54 observed in MSCs cultured with HTLV-1-irradiated cells and in MSCs cultured with cell-free HTLV-1 were similar (Fig. 2A and B). We also observed that the expression of aminopeptidase N (CD13) was 1.3-fold lower in MSCs cultured with irradiated MT2 cells ($p=0.007$; Fig. 2C). The expression of the MHC class II cell surface receptor (HLA-DR) protein was 7.7-fold higher in the same cell population ($p=0.0006$). It is important to note that this difference was observed only between MSCs that had direct contact with HTLV-1-infected-cells and MSCs cultured in the absence of HTLV-1 (Fig. 2C and D). Significant differences were also observed in the expression of the NGF receptor p75NTR protein (CD271), which was reduced (2.5-fold) in MSCs cultured with cell-free concentrated HTLV-1 ($p=0.0247$) compared with MSC control cultures (Fig. 2E). The expression levels of HLA-ABC, CD73, endoglin (CD105), and CD45 were similar ($p > 0.05$) in MSC control cultures and MSCs exposed to HTLV-1 (Supplementary material 1 A–D).

The variations observed in the expression of the surface molecules CD106, CD54, and CD271 were also evaluated by qPCR. The transwell culture resulted in an increase of 5.3- to 2.3-fold in the mRNA expression levels of CD106 and CD54 on MSCs (Supplementary material 2A and 2B). The most significant increase was obtained in the presence of cell-free HTLV-1 and through the direct contact of infected cells and MSCs (6.8- to 18-fold). We also observed that the CD271 gene expression was downregulated (4.5-fold) in MSCs cultured in the presence of HTLV-1 compared with MSCs cultured without HTLV-1 (Supplementary material 2C).

MSC immunophenotypic characteristics are altered by PBMCs from HTLV individuals

Because the group of HTLV-1-infected individuals is composed of both asymptomatic and symptomatic individuals, we examined

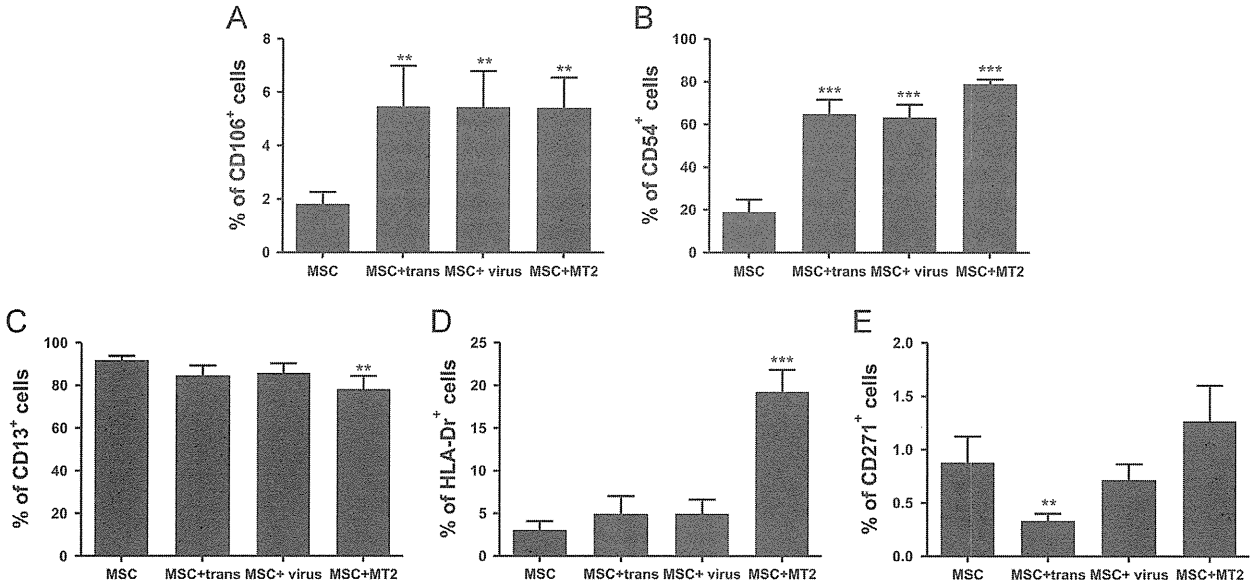

Fig. 2. Effect of HTLV-1 on MSC surface molecule expression. MSCs were cultured for 18 h under different growing conditions: control bone marrow (BM)-mesenchymal stromal cells (MSCs), MSCs cultured with MT2 cells using a transwell system (MSC+trans), MSCs cultured with cell-free HTLV-1 particles (MSC+virus), and MSCs cultured in the presence of irradiated MT2 cells (MSC+MT2). The data are presented as the means ± SEM of the percentage of cells stained with (A) anti-CD106, (B) anti-CD54, (C) anti-CD13, (D) anti-HLA-DR, and (E) anti-CD271, as evaluated by flow cytometry. The results were obtained from at least three independent experiments and evaluated using a one-tail Mann–Whitney *t* test. The asterisks denote significant differences compared with the MSC control culture ($^{*}p < 0.05$, $^{**}p < 0.01$, and $^{***}p < 0.001$).

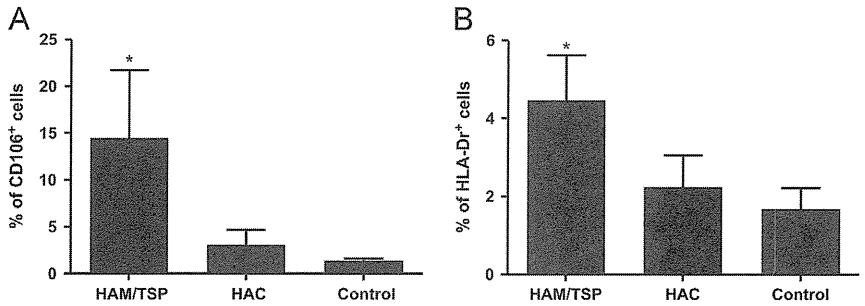

Fig. 3. Immunophenotypic profile of MSCs co-cultured with PBMCs from HTLV-1-infected individuals. MSCs were cultivated with PBMCs isolated from HTLV-1-infected symptomatic individuals (human T lymphotropic virus type 1 (HTLV-1) associated myelopathy/tropical spastic paraparesis; HAM/TSP), asymptomatic HTLV-1 carriers (HAC), and healthy subjects (control) using a transwell system. The data are presented as the means ± SEM of the percentage of cells stained with (A) anti-CD106, (B) anti-CD54, (C) anti-CD271, and (D) anti-HLA-DR antibodies, as evaluated by flow cytometry. The results were obtained from three independent experiments. We used the Mann–Whitney one-tail *t* test. $^{*}p < 0.05$ compared with healthy subjects (control).

whether the PBMCs isolated from these individuals can modulate the expression of adhesion molecules (CD106 and CD54), HLA-DR, and CD271 in MSCs. All of the individuals included in this assay exhibited a $CD4^+/CD8^+$ ratio within the normal limits. As shown in Fig. 3, CD106 was overexpressed (10-fold) in the MSCs cultured with PBMCs from the HTLV-1 symptomatic group compared with MSCs cultured with cells obtained from healthy subjects or asymptomatic infected individuals ($p=0.0189$; Fig. 3A). The expression of HLA-DR was 2.6-fold higher in MSCs cultured with PBMCs isolated from HTLV-1 symptomatic individuals compared with that obtained in MSCs cultured with cells from healthy subjects or asymptomatic infected individuals ($p=0.0175$; Fig. 3B). The CD54 and CD271 expression levels showed no differences between MSCs cultured with PBMCs from HTLV-1-infected individuals or from healthy subjects (Data not shown).

HTLV-1 exposure does not alter the MSC differentiation potential

We also evaluated the effect of HTLV-1 on the MSC ability to differentiate into adipocytes and osteocytes. For this purpose, MSCs were cultivated with virus particles (using a transwell system or cell-free concentrated HTLV-1) or directly co-cultured with irradiated MT2 cells for a period of 18 h. After this period, the MSCs were differentiated into adipocytes and osteocytes for 22 days using the appropriate induction culture medium. In response to adipogenic differentiation, we observed changes in the cell morphology and the formation of lipid vacuoles, as visualized through Sudan II/Scarlet staining, regardless of the presence or absence of HTLV-1 (Fig. 4C, E, G, and I). The analysis of the peroxisome proliferator-activated receptor gamma (*PPAR-γ*) gene expression showed a 70-fold increase in MSCs subjected to

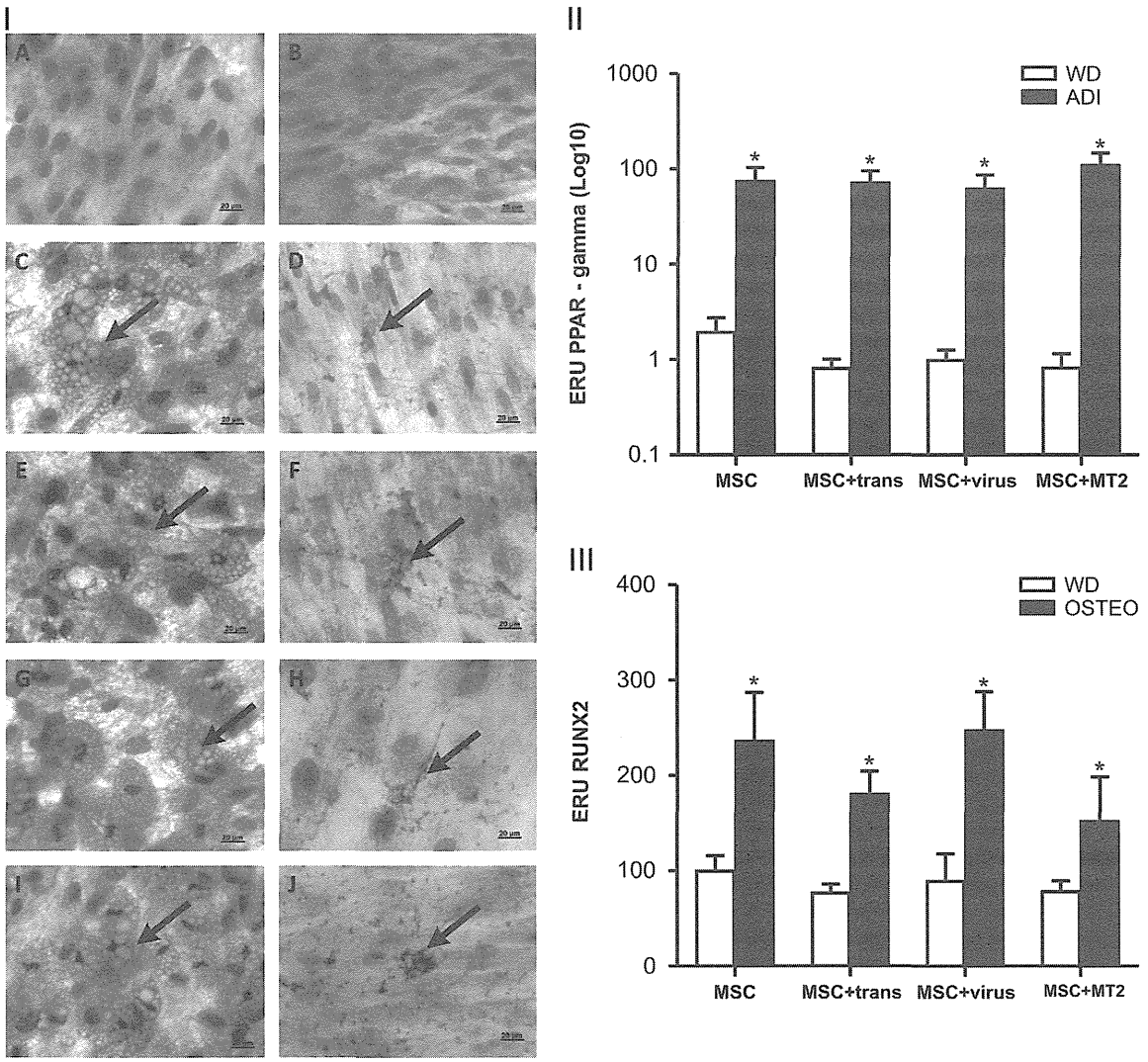

Fig. 4. Adipogenic and osteogenic differentiation of MSCs exposed to HTLV-1. (I) Morphologic analyses of bone marrow (BM)-mesenchymal stromal cells (MSCs) cultured for 18 h in the presence or absence of HTLV-1. MSCs were stained by Sudan II/Scarlet (C, E, G, and I) and the von Kossa method (D, F, H, and J) to evaluate the adipogenic and osteogenic differentiation potential, respectively. (A and B) Control MSCs cultured on standard medium; (C and D) control MSCs; (E and F) MSCs cultured with MT2 cells using a transwell system; (G and H) MSCs cultured with cell-free HTLV-1 particles; and (I and J) MSCs cultured in the presence of irradiated MT2 cells. The arrows indicate lipid vacuoles (C, E, G, and I) and mineralization nodules (D, F, H, and J). The scale bars represent 20 μm. (II) PPARγ gene expression in MSCs during adipogenic differentiation, as determined by qRT-PCR. (III) Level of Runx2 gene expression during osteoblastic differentiation, as determined by qRT-PCR. Control mesenchymal stromal cells (MSCs), MSCs cultured with MT2 cells in a transwell system (MSC+trans), MSCs cultured with cell-free HTLV-1 particles (MSC+virus), and MSCs cultured in the presence of irradiated MT2 cells (MSC+MT2). ADI: adipogenic induction; WD: without differentiation induction; OSTEO: osteogenic induction. The data are reported using expression relative units (ERU), and the results are represented as the means ± SEM ($n=4$ per group). The asterisks denote significant differences relative to the undifferentiated control ($^*p \leq 0.05$).

adipogenic differentiation compared to non-induced MSC. However, the comparison of MSCs cultured in the presence of HTLV-1 and the MSC control culture revealed no significant difference in the mRNA expression of the *PPAR-γ* gene (Fig. 4II).

To further evaluate the effect of HTLV-1 infection on osteogenesis, we compared MSC control cultures and MSCs exposed to HTLV-1. The osteogenic differentiation potential of MSCs was not altered by HTLV-1, and the analyses of calcium deposition and mineralization of the extracellular matrix indicated that there were no significant differences in osteogenic differentiation potential of the studied samples (Fig. 4D, F, H, and J). The analysis of the mRNA expression of the runt-related transcription factor 2 (*RUNX2*) gene revealed that this gene was 2.4-fold overexpressed in MSCs undergoing differentiation into osteocytes than in non-differentiated MSC. However, the *RUNX2* expression level in MSCs that had contact with HTLV-1 was similar to that found in the MSC control culture, indicating that HTLV-1 does not alter the differentiation potential of MSCs into osteocytes (Fig. 4III). These results suggest that HTLV-1 does not modify the differentiation potential of MSCs into adipocytes and osteocytes.

MSCs are susceptible to HTLV-1 infection

Because HTLV-1 infects various cell types, we questioned whether MSCs are susceptible to HTLV-1 infection *in vitro*. First, we evaluated the expression of genes encoding proteins for HTLV-1 receptors, such as *GLUT1*, *HSPG*, and *NRP1*. These gene products are involved in the initial interaction between the cell and the virus and are required for HTLV-1 infection in different cell types. MSCs isolated from the BM of healthy individuals exhibited a *GLUT1* gene expression level similar to that obtained in $CD4^+$ T cells from healthy individuals and $CD4^+$ T cells from HTLV-1-infected individuals; however, the *HSPG* gene was overexpressed (37-fold) in MSCs compared with $CD4^+$ T cells from HTLV-1 individuals ($p=0.0022$). The expression level of the *NRP1* gene was 11-fold higher in $CD4^+$ T cells from HTLV-1 individuals compared with $CD4^+$ T cells from healthy individuals ($p=0.004$); however, *NRP-1* presented higher expression levels in MSCs (Fig. 5).

To evaluate whether the contact of HTLV-1 with MSCs allows the efficient infection of MSCs, we investigated the presence of HTLV-1 provirus in DNA samples extracted from MSCs exposed to HTLV-1. We observed the amplification of the HTLV-1 *Tax* gene by PCR only in MSCs that were cultured with irradiated MT2 cells. No amplification was observed in MSCs grown with cell-free HTLV-1 particles and in the MSC control cultures (Fig. 6I). The results obtained by PCR corroborated the analyses of the expression levels of HTLV-1 proteins. As shown in Fig. 6II (E and F), MSCs cultured with MT2 cells are positive for the HTLV-1 p19 protein, as evidenced by confocal microscopy analyses (Fig. 6IIE and 6IIF). No evidence of the p19 specific signal was observed in the control cultures (Fig. 6IIH and III). The HTLV-1 Tax regulatory protein was also detected in MSCs co-cultured with MT2 cells by flow cytometry, which suggests that HTLV-1 results in productive infection and viral replication in MSCs (Fig. 6IV).

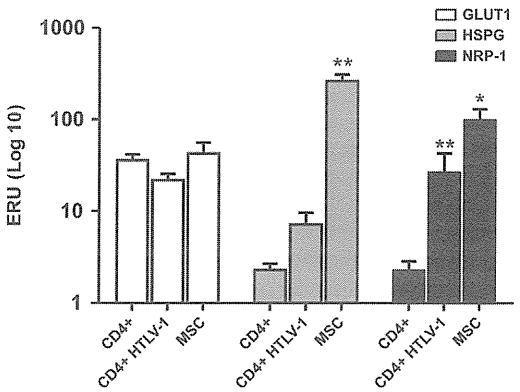

Fig. 5. Gene expression of HTLV-1 receptors in different cell types. Quantification by real-time PCR of the mRNA levels of *GLUT1*, *HSPG*, and *NRP-1* in $CD4^+$ T cells and MSCs isolated from healthy individuals and HTLV-1-infected individuals. The data are reported as expression relative units (ERU) and represent the means ± SEM of triplicate experiments. We used a one-tail Mann–Whitney *t* test, and the asterisks denote significant differences compared with $CD4^+$ T cells ($^*p<0.05$ and $^{**}p<0.01$).

Discussion

HTLV-1 is a retrovirus that primarily infects T cells and is able to establish lifelong latency in its host. Although the great majority of HTLV-1-infected individuals remain asymptomatic, a minor group of patients develops one of two main disorders, namely HAM/TSP and ATLL, and other clinical manifestations, such as uveitis, arthritis, and infectious dermatitis (Oh and Jacobson, 2008; Yoshida et al., 1984; LaGrenade et al., 1990; Mariette et al., 2000). Various factors, such as the proviral load and the effectiveness of the immune response, are considered important factors that determine the risk of developing clinical diseases (Manns et al., 1999; Montanheiro et al., 2005).

In contrast, the immunomodulation properties of MSCs can exert an effective inhibitory effect on the function of immune cells and thus provide an interesting therapeutic tool for the treatment of degenerative disorders, as well as inflammatory and autoimmune diseases (Di Nicola et al., 2002; Bartholomew et al., 2002). Several studies have reported that the role of MSCs can be modulated by inflammatory mediators released from activated immune cells (Waterman et al., 2010; Auletta et al., 2012). Thus, the exposure of MSCs to an infectious or inflammatory microenvironment could alter their functions and change their differentiation potential and interaction with immune cells.

In this study, we present data that demonstrate the influence of HTLV-1 on the biological and functional features of BM-derived MSCs. Our results showed that MSCs exposed to HTLV-1 display distinct characteristics from those of MSCs cultured under control conditions. For example, contact with HTLV-1 resulted in the accumulation of vesicles in the cytosol of MSCs, and this phenomenon is similar to that observed when HTLV-1 infects HeLa cells, Jurkat cells, and human primary PBMCs (autophagic vacuoles). This accumulation of autophagosomes is induced by the HTLV-1 Tax protein and benefits virus replication (Tang et al., 2013).

Surface molecules, such as ICAM-1, VCAM-1, and HLA-DR, were found to be upregulated in MSCs after contact with HTLV-1. In addition, PBMCs isolated from HTLV-1 symptomatic individuals were also able to modulate the expression of VCAM1 and HLA-DR in MSCs, even without direct cell contact.

The cell surface glycoproteins ICAM-1 and VCAM-1 are members of the immunoglobulin superfamily that are closely related to the processes of recognition, interaction, and adhesion. The expression of ICAM-1 and VCAM-1 first occurs in endothelial cells and immune system cells; however, previous studies have described that MSCs may produce large amount of chemokines and adhesion molecules after stimulation with inflammatory cytokines (Ren et al., 2008, 2010). Moreover, the serum of HAM/TSP individuals shows a higher concentration of pro-inflammatory cytokines, such as TNF-α, IL-6 and IFN-γ, compared with that of asymptomatic individuals, and these cytokines can modulate the MSC adhesion molecules (Starling et al., 2013). Other studies have shown that MSC activity can be modulated differently depending on the environment. Viral infections are stimuli that can enhance the immunosuppressive capacity promoted by MSCs due to an increase in the expression of

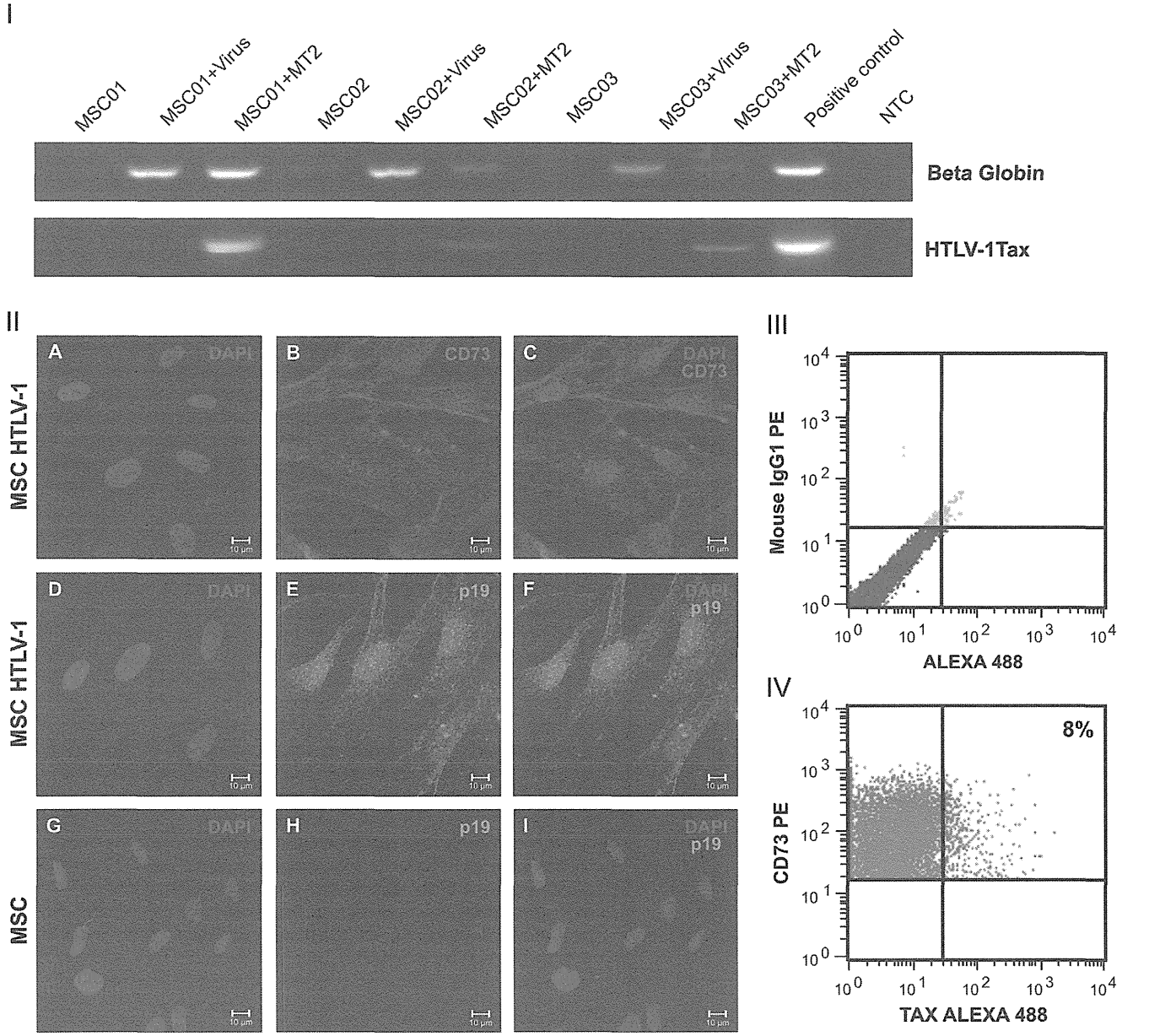

Fig. 6. HTLV-1 infection in MSCs. (I) Human β-globin and HTLV-1 tax gene amplification by PCR. The results were obtained from three independent experiments. Control mesenchymal stromal cells (MSC01, MSC02, and MSC03), MSCs cultured with cell-free HTLV-1 particles (MSC01+virus, MSC02+virus, and MSC03+virus), and MSCs cultured in the presence of irradiated MT2 cells (MSC01+MT2, MSC01+MT2, and MSC01+MT2), MT2 DNA (positive control), and no template control (NTC). (II) Representative immunofluorescence staining of mesenchymal stromal cells. (A) MSCs co-cultured with MT2 cells were stained with DAPI (blue) and (B) anti-CD73 (red); (C) overlap of DAPI (blue) and anti-CD73 (red) staining. MSCs co-cultured with MT2 cells were stained with (D) DAPI (blue) and (E) anti-CD19 (green); (F) overlap of DAPI (blue) and anti-CD19 (green) staining. The nucleus of control MSCs were stained with (G) DAPI (blue) and (H) anti-CD19 (green); (I) overlap of DAPI (blue) and anti-CD19 (green) staining. The scale bars represent 10 μm. (III and IV) Representative flow cytometry dot plots of MSCs co-cultured with MT2 cells. (III) Isotype-matched control antibodies. (IV) The dots in the upper right quadrant of the flow plot represent cells that coexpress CD73 and the HTLV-1 tax protein (8%).

adhesion molecules (ICAM-1 and VCAM-1) (Ren et al., 2010). Therefore, MSCs exposed to HTLV-1 should also induce a differentiated immunosuppressive effect on T lymphocytes because ICAM-1 and VCAM-1 expression modulate the immune regulatory properties of MSCs.

According to the literature, a significant increase in the expression levels of ICAM-1 (CD54) and LFA-3 (CD58) has been described in MSCs in response to CMV infection, and this increase is associated with a higher adherence of hematopoietic cells to CMV-infected MSCs (Smirnov et al., 2007). Previous studies have demonstrated that, in HTLV-1 infection, ICAM-1 and LFA-1 are modulated in T cells (Barnard et al., 2005), and these interactions are important for cell fusion and the dissemination of HTLV-1, thereby allowing an improvement of the cell-cell contact, the polarization of the cytoskeleton, and the formation of a viral synapse (Igakura et al., 2003). However, the increased expression of adhesion molecules (ICAM-1 and VCAM-1) in MSCs exposed to HTLV-1 suggests that the contact between infected cells and MSCs is favored and may also promote the HTLV-1 infection of MSCs and BM resident cells.

With respect to the expression of HLA-DR, some researchers have shown that the expression of HLA-DR in MSCs depends on the IFN-γ concentration. Upon exposure to antigens, the initial doses of IFN-γ induce the expression of MHC-II molecules and

thereby facilitate the antigen presenting properties of MSCs. However, at high levels of IFN-γ, the MHC-II expression is down-regulated, which causes a loss in the ability of MSCs to act as antigen presenting cells (APCs) (Stagg et al., 2006; Romieu-Mourez et al., 2007).

Other typical surface molecules that are commonly used in the characterization of MSC, such as CD271 and CD13, were also modulated by HTLV-1 contact. However, further studies should be conducted to understand the differences in the expression of these molecules in MSCs exposed to HTLV-1 because no studies have reported the involvement of CD271 in virus infection and CD13 expression is considered important in other infections, e.g., in CMV infection, CD13 is reported to act as a receptor (Soderberg et al., 1993).

The functional capacity of MSCs to differentiate into adipocytes and osteocytes was not altered in MSCs exposed to HTLV-1, and this finding was confirmed by the analysis of the gene expression levels of PPARγ and RUNX-2. Previous reports have described that HTLV-1 may be linked to bone alteration by increasing the population of active osteoclasts in ATLL patients (Kiyokawa et al., 1987). This change is likely not related to HTLV-1-exposed MSCs because we observed that HTLV-1 did not impair the osteogenic differentiation potential of this cell population. It is believed that the alterations observed in the osteoclasts of ATLL cells and HTLV-1-infected T cells maintained in culture may arise due to the overexpression and secretion of specific cytokines that stimulate the proliferation of osteoclast precursors and promote their differentiation (Tendler et al., 1991).

Other authors who assessed the MSC differentiation potential during HIV infection showed that the p55-gag viral protein affects osteogenesis by reducing calcium deposition and the expression and activity levels of RUNX-2. However, the cell lipid levels and PPARγ activity were increased by HIV proteins during adipogenic MSC differentiation (Cotter et al., 2008, 2011, 2007). Experiments performed with sera from high-viral-load HIV-infected individuals induced a proadipogenic phenotype, as evidenced by the increased adipocyte formation and the expression of PPARγ (Cotter et al., 2011). HIV infection has also been found to affect the proliferation and osteogenic differentiation of MSCs isolated from Tg26 HIV-1 mice, which suggests that the infection progressively causes damage to MSC functionality (Cheng et al., 2013).

Our results also provide the first demonstration that the interaction between HTLV-1 and BM-derived MSCs leads to their infection *in vitro*. In fact, the presence of HTLV-1 integrated provirus was evidenced only in MSCs that had direct contact with an infected cell and not with cell-free virions, which shows that direct contact with an infected cell is efficient for the virus infection of MSCs. These findings support the hypothesis that the main transmission route for HTLV-1 infection first occurs through cell-to-cell contact because cell-free virions are very poorly infectious *in vitro* (Donegan et al., 1994). However, in other cell types, such as DCs, efficient and productive infection has been observed with cell-free HTLV-1 (Jones et al., 2008).

The existence of HTLV-1-infected cells in the BM had been explored in *in vivo* studies on ATLL patients, and the results have shown that HTLV-1 DNA is detected in BM mononuclear cells but not in hematopoietic stem cells ($CD34^+$) (Nagafuji et al., 1993). An extensive latent infection in the BM of patients with HTLV-1 has also been demonstrated; however, the phenotype of HTLV-1-infected BM cells is unclear (Jacobson et al., 1997). We suggest the biological existence of HTLV-1-infected MSCs in the BM of HTLV-1-infected individuals; however, further studies are necessary to detect the productive infection of MSCs isolated from HTLV-1-infected individuals.

Others studies have previously been performed to elucidate the susceptibility of MSCs to virus infection and the possible consequences of the contact of MSCs with infectious agents. Herpes virus (HSV-1) was found to be able to infect MSCs *in vitro* and induces a cytopathic effect, as evidenced by signs of swelling and detachment from walls (Sundin et al., 2006). Recently, Avanzi et al. (2013) demonstrated that fetal membrane (FM) derived-MSCs (FM-MSCs) are fully permissive to infection with herpes simplex virus 1 and 2 (HSV-1 and HSV-2), varicella zoster virus (VZV), and human cytomegalovirus (HCMV) but not with Epstein-Barr virus (EBV) and human herpes virus 6, 7, and 8 (HHV-6, 7, and 8). Although these viruses are capable of entering FM-MSCs, transient and limited viral gene expression occurs (Avanzi et al., 2013).

Conclusion

In conclusion, we have shown that HTLV-1 modifies important MSC characteristics, such as the formation of intracellular vesicle structures and the expression of the surface molecules ICAM-1, VCAM-1, and HLA-DR. However, the MSC ability to differentiate into adipocytes and osteocytes was not affected by HTLV-1. In addition, MSCs were found to be susceptible to HTLV-1 infection *in vitro*, and this finding was supported by the hypothesis that, as part of the regular immune surveillance process, HTLV-1-infected $CD4^+$ and $CD8^+$ T cells are able to traffic during primary infection and viral latency into the BM, where cell-to-cell contact over a prolonged period of time can lead to progressive HTLV-1 BM invasion and probable infection of BM resident cells (Grant et al., 2002). Understanding the biological mechanisms involved during HTLV-1 infection and knowing the target cells and the possible routes of HTLV-1 spread in the body may aid the development of an appropriate and effective management strategy for this infection that improves the quality of life of HTLV-1-infected individuals.

Methods

HTLV-1-seropositive individuals

HTLV-1-seropositive individuals were diagnosed from blood-donor candidates of the Regional Blood Center of Ribeirão Preto. Samples were also collected from HTLV-1-infected individuals belonging to the Neurology Department of the University Hospital, São Paulo, Brazil. The diagnosis of HTLV-1/2 infection was established by an antibody screening of serum/plasma samples using an enzyme immunoassay (EIA; ORTHO HTLV-1/2 Ab-capture ELISA test system, Ortho Clinical Diagnostics, Inc., Raritan, N, USA) followed by PCR confirmation using amplification primers for the *tax* and *LTR* regions of HTLV-1 and the *LTR* and *pX* regions of HTLV-2 according to previously described protocols (Pinto et al., 2012). The HTLV-1 group consisted of seven individuals classified as healthy asymptomatic HTLV-1 carriers (HAC; 57.1% females, 42.9% males; mean age=46.2 years) and six individuals with HAM/TSP (83.3% females, 16.7% males; mean age=51.5 years). The mean HTLV-1 proviral load was 2190.8 copies/10^5 cells for HAC individuals and 7214.9 for HAM/TSP individuals. The healthy control group consisted of seven randomly selected blood donors from the same geographical region as the HTLV-1-positive individuals described above, and these had a mean age of 44.7 years (85.7% females, 14.3% males). This study was approved by the Institutional Ethics Committee at the General Hospital of the Faculty of Medicine in Ribeirão Preto, University of São Paulo, Brazil (Process number 12462/2010). All of the patients enrolled in this study signed a written informed consent form.

Isolation, culture, and characterization of the cells

Peripheral blood mononuclear cells (PBMCs). PBMCs were separated from the whole blood using Ficoll-Paque™ PLUS (GE Healthcare Biosciences, Uppland, Sweden) according to the

manufacturer's instructions. The T cells phenotypic analysis for $CD3^+$, $CD8^+$, $CD45^+$, and $CD4^+$ was performed by flow cytometry (BD Multitest™, BD Biosciences, CA, USA). Immunomagnetic cell separation was performed to obtain $CD4^+$ T cells (CD4 MicroBeads MACs Miltenyi Biotec, CA, USA).

MSC isolation. Approximately 10 mL of human bone marrow aspirates were collected from healthy donors. The mononuclear cells were separated by Ficoll-Paque™ PLUS (GE Healthcare Biosciences, Uppland, Sweden), and the MSCs were isolated by plastic adherence and cultured at a concentration of $2–4 \times 10^5$ cells/mL in 25-cm^2 flasks (Corning, NY, USA) with alpha minimum essential medium (α-MEM) (Gibco, NY, USA) supplemented with 15% heat-inactivated standard fetal bovine serum (HyClone, UT, USA), 2 mM L-glutamine (Gibco, Grand Island, NY, USA), and 1% penicillin–streptomycin (Gibco, NY, USA). The non-adherent T cells were removed after 72 h, and the formation of colonies was observed after 3 to 4 days. The plastic-adherent MSCs at passages 3–5 were used in the experiments. The cultured MSCs were immunophenotypically characterized using the following monoclonal antibodies: CD45-FITC (fluorescein isothiocyanate), CD31-FITC, HLA-DR-FITC, CD73-PE (phycoerythrin), CD146-FITC, CD90-PE, CD29-APC (allophycocyanin), CD44-FITC, CD13-PE, CD49e-PE, HLA-ABC-PE, CD34-APC, CD14-PE, CD54-PE, CD166-PE, and CD105-PerCP (peridinin chlorophyll protein complex) (BD Biosciences, CA, USA). The adipogenic, osteogenic, and chondrogenic MSC differentiation potential were evaluated as described below.

Cell lines. MT2 cells (HTLV-1-infected cell line) were cultured in RPMI (Gibco, NY, USA) supplemented with 10% fetal bovine serum and 1% penicillin–streptomycin (Gibco, NY, USA). All of the cultures were maintained in a humidified atmosphere of 5% CO_2 at 37 °C.

Virus infection and co-culture assay

The HTLV-1 concentration was determined according to the following protocol. MT2 cells were cultured (1×10^7) in complete RPMI medium for 24 h. The viral supernatant was collected, filtered through a 45-μm filter (Millipore, MA, USA), and ultracentrifuged at 10,000*g* for 2 h. The concentrated virus was quantified through p19 enzyme immunoassay (EIA) (ZeptoMetrix Corporation, NY, USA) according to the manufacturer's instructions and stored at −80 °C. The ability of HTLV-1 to infect MSCs was examined using concentrated virus and co-culture assays. Human MSCs (2.5×10^3) at passages 3–5 were seeded into individual wells of a six-well culture plates for 24 h. Concentrated HTLV-1 (100 ng) was added to the MSC culture and maintained for 18 h. For the co-culture assay, MSCs were cultured in complete RPMI medium at 37 °C for 18 h with MT2 cells irradiated with 60,000 Gy at a ratio of 1:1 or with MT2 cells in a transwell system (Greiner Bio-one, NC, USA). As a control, we maintained cells in the same medium without addition of the virus. The experiments were repeated at least three times, and the results were calculated as the means ± SEM of triplicates.

Electron microscopy

MSCs co-cultured with MT2 cells for 18 h were fixed with 2.0% glutaraldehyde and 2% paraformaldehyde in 0.1 M (pH 7.2) cacodylate buffer supplemented with 5 mM $MgCl_2$, 5 mM $CaCl_2$, and 0.1 M sucrose. The filters were washed in cacodylate buffer and postfixed for 1 h at room temperature in 1% osmium tetroxide solution. The samples were washed three times in water and incubated in 0.5% uracil acetate. The cells were dehydrated in an ethanol gradient (from 25 to 100%) and embedded into epoxy resin at 60 °C for 48 h. After washing in propylene oxide, ultrathin sections were cut using a Leica Ultracut S microtome. The sections were then examined using a JEOL JEM-100 CX II electron microscope.

Immunocytochemistry assay

Immunocytochemistry was performed to confirm the HTLV-1 infection of MSCs. MSCs co-cultured with MT2 cells (2×10^4) or under control conditions were seeded on glass coverslips (Gold-Lab, SP, Brazil) in 24-well plates (Corning, NY, USA) and incubated until the cells reached 80% confluence. The cells were fixed in 4% paraformaldehyde (Merck, NJ, USA) for 20 min at room temperature, washed three times with PBS, and then permeabilized with 0.2% Triton X-100 (Sigma-Aldrich, MO, USA) for 1 h at room temperature. The cells were blocked for 1 h with 5% bovine serum albumin (BSA) and 2% goat serum diluted in PBS. The samples were separately incubated with primary anti-HTLV-1 p19 antibodies (Abcam, MA, USA) and CD73 (BD Pharmingen, CA, USA) at room temperature overnight. The secondary antibody used was Alexa Fluor 488 mouse antibody (Invitrogen, CA, USA). The nuclei were stained with DAPI (Vysis, IL, USA). The cells were visualized separately using a confocal laser scanning microscope (CLSM) (LSM 710; Carl Zeiss, Germany) with 20x and 63x objective lenses and a numerical aperture of 1.4. An argon 488-nm laser was used to excite the fluorochrome of the secondary antibodies, and the emission was measured at 525 nm. The visualization of the light scattering for each excitation wavelength was recorded in the multitracking mode using separate detection channels. The image analysis was performed using the ZEN2008 software (Carl Zeiss, Germany). The control and test images were captured using identical settings.

Flow cytometry analysis

The cultured MSCs were immunophenotypically characterized by flow cytometry using the following monoclonal antibodies: CD106 (VCAM1, vascular cell adhesion molecule 1)-PE, CD54 (ICAM-1, type I transmembrane protein)-PE, CD13-APC, HLA-DR (major histocompatibility complex, class II)-PE, CD271 (NGFR, nerve growth factor receptor)-PE, HLA-ABC-PE, CD73 (NT5E, 5-nucleotidase, ecto)-PE, CD105 (ENG, endoglin)-PerCP, and CD45 (Leukocyte common antigen)-FITC (BD Biosciences, CA, USA).

For the intracellular detection of *tax*, the cells were fixed in 1% paraformaldehyde (Sigma-Aldrich, MO, USA), permeabilized with 1% Tween 20, and stained with a specific antibody (kindly provided by Dr. Yuetsu Tanaka, University of the Ryukyus, Okinawa, Japan). For the analysis of the surface epitope by FACS, the cells were incubated with fluorescence-conjugated antibodies (1 μg per 10^6 cells) at room temperature for 30 min. After washing twice with 1X PBS, the cells were suspended in PBS and analyzed using a FACScalibur flow cytometer (BD Biosciences, CA, USA). Ten thousand events were acquired and analyzed using the CellQuest software (BD Biosciences, CA, USA). Nonspecific IgG of the corresponding class served as a negative control.

MSC differentiation into adipocytes and osteocytes

The adipogenic and osteogenic differentiation of MSCs was obtained as described previously (Castilho-Fernandes et al., 2011). In brief, the differentiation was induced after incubation of the cells with specific differentiation media for adipocytes (α-MEM (Gibco-Invitrogen, CA, USA) supplemented with 15% FBS (Thermo Scientific HyClone, UT, USA), 1 mM dexamethasone (Dex; Sigma-Aldrich, MO, USA), 2.5 mg/mL insulin, and 0.5 mM isobutylmethylxanthine (Sigma-Aldrich, MO, USA)) and for osteocytes (α-MEM (Gibco-Invitrogen, CA, USA) supplemented with 7.5% FBS (Thermo

Scientific HyClone, UT, USA), 0.1 mM Dex (Sigma-Aldrich, MO, USA), 20 mM ascorbic acid, and 1 M β-glycerophosphate (Sigma-Aldrich, MO, USA)). The media were replaced every three days over a period of 22 days, and the cells were then fixed and stained through the von Kossa method (for calcium deposition) with Sudan II and Scarlet stains (for accumulation of fat). The control cells were maintained in standard α-MEM (Gibco, Invitrogen, CA, USA) with 7.5% fetal bovine serum (Thermo Scientific HyClone, UT, USA) over the same period. The cells were analyzed using an AxioScope 2.0 Zeiss microscope equipped with an AxioCam HR (Carl Zeiss, Jena, Germany) and by real-time PCR for the gene expression.

Quantitative real-time PCR (qRT-PCR)

The total cell RNA was extracted using an RNeasy mini kit (Qiagen, North Rhine-Westphalia, Germany) according to manufacturer's instructions and stored at −80 °C. The quantity and quality of the RNA were assessed by spectrophotometry using a Nanodrop instrument (Thermo Fisher Scientific, NJ, USA). The complementary DNA (cDNA) was synthesized from 1 μg of total RNA using a high-capacity cDNA archive kit (Applied Biosystems, CA, USA). The cDNA was diluted 10 times in nuclease-free water and was used in each real-time PCR reaction. The SYBR® Green PCR mix (Applied Biosystems, CA, USA) was used to determine the gene expression of HTLV-1 receptors using the following primers: NRP1F, 5′-CCTGAATGTTCCCAGAACTACACAA-3′; NRP1R, 5′-CAACATCAGGGAATCCATCCC-3′; HSPG2F, 5′-TGGACACATTCGTACCTTTCTGA-3′; HSPG2R, 5′-ACTCCGACTCCAGCGTGTCT-3′; GLUT1F, 5′-atggagcca gcagcaagaa-3′; GLUT1R, 5′-agggaccagagcgtggtgag-3′. We also evaluated the gene expression of PPARγ using the following primers: PPARF, 5′-TCCCGCTGACCAAAGCAAG-3′; PPARR, 5′-CAGGGGGGTGATGTG TTTGA-3′. The endogenous controls were human actin beta (ACTB; ACTBF, 5′-GCCCTGAGGCACTCTTCCA-3′; ACTBR, 5′-CCAGGGCAGTGATCTCCTTCT-3′) and glyceraldehyde-3-phosphate dehydrogenase (GAPDH; GAPDHF, 5′-GCCTCAAGATCATCAGCAATGC-3′; GAPDHR, 5′-CATGGACTGTGGTCATGAGTCCT-3′). The single-product amplification was confirmed by the post-melting curve.

The quantitative RT-PCR was performed using TaqMan™ assays for the *tax* and *env* HTLV-1 genes (specific probe FAM labeled), RUNX2 (Hs00231692_m1), CD106 (Hs00174239_m1), CD54 (Hs00164932_m1), and CD271 (Hs00609977_m1; Applied Biosystems, CA, USA). The reaction was performed in a final volume of 15 μL for 40 cycles under universal cycling conditions (40 cycles of 95 °C for 15 s and 60 °C for 1 min) in an ABI Prism 7500 sequence detection system (Applied Biosystems, CA, USA). The results were normalized using the geometric mean of the endogenous genes GAPDH, ACTB, and B_2 microglobulin (B2M). Duplicate samples were measured and averaged. The results are reported using expression relative units (Albesiano et al., 2003). The HTLV-I proviral load was determined using the *pol* HTLV-1 and ACTB genes.

Statistical analysis

The assays were conducted in at least triplicate. To evaluate the differences between MSCs cultured under control conditions and MSCs exposed to HTLV-1, we used the Mann–Whitney *t* test. The results are expressed as the means ± SEM. The statistical analysis was performed using GraphPad Prism (version 5.0; La Jolla, CA, USA), and differences were considered statistically significant if $^{*}p < 0.05$, $^{**}p < 0.01$, and $^{***}p < 0.001$.

Authors' contribution

Rodrigues E.S. was responsible for experimental design, cell cultures and statistics analyses, Macedo M.D. was responsible for cell cultures, Pinto M.T. was responsible for $CD4^+$ T cells isolation and reverse transcription, Orellana M.D. was responsible for MSC isolations, Rocha-Junior M.C. conducted HTLV-1 particles concentration, Magalhães D.A.R. conducted immunocytochemistry assay, Takayanagui O.M. was responsible for HTLV-1 individuals assistance, Covas D.T. and Kashima S were responsible for the overall experimental design and coordination of the project.

Acknowledgments

This study was supported by CNPq Universal (Process number 477126/2009-0). Center for Cell-based Therapy (CTC), Fundação de Amparo à Pesquisa do Estado de São Paulo (FAPESP) and Fundação Hemocentro de Ribeirão Preto (FUNDHERP). We are grateful to the staff and blood donors of Regional Blood Center of Ribeirão Preto and patients from the Neurology Department of the University Hospital. The authors thank Leonardo Lira do Amaral for the assistance in cell irradiation and Patrícia Vianna Bonini Palma for cytometry analyses. The authors acknowledge Svetoslav Nanev Slavov for scientific contribution and Fernanda Udinal for English language support. We also thank Sandra Navarro Bresciani for preparing the figures and Josiane Serrano Borges for technical support with glass coverslips.

Appendix A. Supporting information

Supplementary data associated with this article can be found in the online version at http://dx.doi.org/10.1016/j.virol.2013.11.022.

References

Albesiano, E., Messmer, B.T., Damle, R.N., Allen, S.L., Rai, K.R., Chiorazzi, N., 2003. Activation-induced cytidine deaminase in chronic lymphocytic leukemia B cells: expression as multiple forms in a dynamic, variably sized fraction of the clone. Blood 102, 3333–3339.

Araújo, A.Q., Leite, A.C., Dultra, S.V., Andrada-Serpa, M.J., 1995. Progression of neurological disability in HTLV-I-associated myelopathy/tropical spastic paraparesis (HAM/TSP). J. Neurol. Sci. 129, 147–151.

Auletta, J.J., Deans, R.J., Bartholomew, A.M., 2012. Emerging roles for multipotent, bone marrow-derived stromal cells in host defense. Blood 119, 1801–1809.

Avanzi, S., Leoni, V., Rotola, A., Alviano, F., Solimando, L., Lanzoni, G., Bonsi, L., Di Luca, D., Marchionni, C., Alvisi, G., Ripalti, A., 2013. Susceptibility of human placenta derived mesenchymal stromal/stem cells to human herpesviruses infection. PLoS One 8 (8), e71412.

Barnard, A.L., Igakura, T., Tanaka, Y., Taylor, G.P., Bangham, C.R., 2005. Engagement of specific T-cell surface molecules regulates cytoskeletal polarization in HTLV-1-infected lymphocytes. Blood 106 (3), 988–995.

Bartholomew, A., Sturgeon, C., Siatskas, M., Ferrer, K., McIntosh, K., Patil, S., Hardy, W., Devine, S., Ucker, D., Deans, R., Moseley, A., Hoffman, R., 2002. Mesenchymal stem cells suppress lymphocyte proliferation in vitro and prolong skin graft survival in vivo. Exp. Hematol. 30, 42–48.

Castilho-Fernandes, A., de Almeida, D.C., Fontes, A.M., Melo, F.U., Picanço-Castro, V., Freitas, M.C., Orellana, M.D., Palma, P.V., Hackett, P.B., Friedman, S.L., Covas, D.T., 2011. Human hepatic stellate cell line (LX-2) exhibits characteristics of bone marrow-derived mesenchymal stem cells. Exp. Mol. Pathol. 91, 664–672.

Cheng, K., Rai, P., Lan, X., Plagov, A., Malhotra, A., Gupta, S., Singhal, P.C., 2013. Bone-derived mesenchymal stromal cells from HIV transgenic mice exhibit altered proliferation, differentiation capacity and paracrine functions along with impaired therapeutic potential in kidney injury. Exp. Cell Res. 319 (14), 2266–2274.

Choudhary, S., Marquez, M., Alencastro, F., Spors, F., Zhao, Y., Tiwari, V., 2011. Herpes simplex virus type-1 (HSV-1) entry into human mesenchymal stem cells is heavily dependent on heparan sulfate. J. Biomed. Biotechnol. 2011, 264350.

Cotter, E.J., Malizia, A.P., Chew, N., Powderly, W.G., Doran, P.P., 2007. HIV proteins regulate bone marker secretion and transcription factor activity in cultured human osteoblasts with consequent potential implications for osteoblast function and development. AIDS Res. Hum. Retroviruses 23, 1521–1530.

Cotter, E.J., Ip, H.S., Powderly, W.G., Doran, P.P., 2008. Mechanism of HIV protein induced modulation of mesenchymal stem cell osteogenic differentiation. BMC Musculoskelet. Disord. 9, 33.
Cotter, E.J., Chew, N., Powderly, W.G., Doran, P.P., 2011. HIV type 1 alters mesenchymal stem cell differentiation potential and cell phenotype ex vivo. AIDS Res. Hum. Retroviruses 27, 187–199.
Di Nicola, M., Carlo-Stella, C., Magni, M., Milanesi, M., Longoni, P.D., Matteucci, P., Grisanti, S., Gianni, A.M., 2002. Human bone marrow stromal cells suppress T-lymphocyte proliferation induced by cellular or nonspecific mitogenic stimuli. Blood 99, 3838–3843.
Dominici, M., Le Blanc, K., Mueller, I., Slaper-Cortenbach, I., Marini, F., Krause, D., Deans, R., Keating, A., Dj, Prockop, Horwitz, E., 2006. Minimal criteria for defining multipotent mesenchymal stromal cells: the International Society for Cellular Therapy position statement. Cytotherapy 8, 315–317.
Donegan, E., Lee, H., Operskalski, E.A., Shaw, G.M., Kleinman, S.H., Busch, M.P., Stevens, C.E., Schiff, E.R., Nowicki, M.J., Hollingsworth, C.G., Mosley, J.W., 1994. Transfusion transmission of retroviruses: human T-lymphotropic virus types I and II compared with human immunodeficiency virus type 1. Transfusion 34, 478–483.
da Silva Meirelles, L., Chagastelles, P.C., Nardi, N.B., 2006. Mesenchymal stem cells reside in virtually all post-natal organs and tissues. J. Cell Sci. 119, 2204–2213.
Friedenstein, A.J., Gorskaja, J.F., Kulagina, N.N., 1976. Fibroblast precursors in normal and irradiated mouse hematopoietic organs. Exp. Hematol. 4, 267–274.
Gibellini, D., Alviano, F., Miserocchi, A., Tazzari, P.L., Ricci, F., Clò, A., Morini, S., Borderi, M., Viale, P., Pasquinelli, G., Pagliaro, P., Bagnara, G.P., Re, M.C., 2011. HIV-1 and recombinant gp120 affect the survival and differentiation of human vessel wall-derived mesenchymal stem cells. Retrovirology 8, 40.
Grant, C., Barmak, K., Alefantis, T., Yao, J., Jacobson, S., Wigdahl, B., 2002. Human T cell leukemia virus type I and neurologic disease: events in bone marrow, peripheral blood, and central nervous system during normal immune surveillance and neuroinflammation. J. Cell. Physiol. 190, 133–159.
Igakura, T., Stinchcombe, J.C., Goon, P.K., Taylor, G.P., Weber, J.N., Griffiths, G.M., Tanaka, Y., Osame, M., Bangham, C.R., 2003. Spread of HTLV-I between lymphocytes by virus-induced polarization of the cytoskeleton. Science 299, 1713–1716.
Jacobson, S., McFarlin, D.E., Robinson, S., Voskuhl, R., Martin, R., Brewah, A., Newell, A.J., Koenig, S., 1992. HTLV-I-specific cytotoxic T lymphocytes in the cerebrospinal fluid of patients with HTLV-I-associated neurological disease. Ann. Neurol. 32, 651–657.
Jacobson, S., Krichavsky, M., Flerlage, N., Levin, M., 1997. Immunopathogenesis of HTLV-I associated neurologic disease: massive latent HTLV-I infection in bone marrow of HAM/TSP patients. Leukemia 11 (Suppl. 3), 73–75.
Jones, K.S., Petrow-Sadowski, C., Huang, Y.K., Bertolette, D.C., Ruscetti, F.W., 2008. Cell-free HTLV-1 infects dendritic cells leading to transmission and transformation of CD4(+) T cells. Nat. Med. 14, 429–436.
Kiyokawa, T., Yamaguchi, K., Takeya, M., Takahashi, K., Watanabe, T., Matsumoto, T., Lee, S.Y., Takatsuki, K., 1987. Hypercalcemia and osteoclast proliferation in adult T-cell leukemia. Cancer 59, 1187–1191.
LaGrenade, L., Hanchard, B., Fletcher, V., Cranston, B., Blattner, W., 1990. Infective dermatitis of Jamaican children: a marker for HTLV-I infection. Lancet 336, 1345–1347.
Manns, A., Miley, W.J., Wilks, R.J., Morgan, O.S., Hanchard, B., Wharfe, G., Cranston, B., Maloney, E., Welles, S.L., Blattner, W.A., Waters, D., 1999. Quantitative proviral DNA and antibody levels in the natural history of HTLV-I infection. J. Infect. Dis. 180, 1487–1493.
Marandin, A., Canque, B., Coulombel, L., Gluckman, J.C., Vainchenker, W., Louache, F., 1995. In vitro infection of bone marrow-adherent cells by human immunodeficiency virus type 1 (HIV-1) does not alter their ability to support hematopoiesis. Virology 213, 245–248.
Mariette, X., Agbalika, F., Zucker-Franklin, D., Clerc, D., Janin, A., Cherot, P., Brouet, J. C., 2000. Detection of the tax gene of HTLV-I in labial salivary glands from patients with Sjögren's syndrome and other diseases of the oral cavity. Clin. Exp. Rheumatol. 18, 341–347.
Montanheiro, P.A., Montanheito, P.A., Oliveira, A.C., et al., 2005. Human T-cell lymphotropic virus type I (HTLV-I) proviral DNA viral load among asymptomatic patients and patients with HTLV-I-associated myelopathy/tropical spastic paraparesis. Braz. J. Med. Biol. Res. 38, 1643–1647.
Nagafuji, K., Harada, M., Teshima, T., et al., 1993. Hematopoietic progenitor cells from patients with adult T-cell leukemia-lymphoma are not infected with human T-cell leukemia virus type 1. Blood 82, 2823–2828.
Nagai, M., Usuku, K., Matsumoto, W., Kodama, D., Takenouchi, N., Moritoyo, T., Hashiguchi, S., Ichinose, M., Bangham, C.R., Izumo, S., Osame, M., 1998. Analysis of HTLV-I proviral load in 202 HAM/TSP patients and 243 asymptomatic HTLV-I carriers: high proviral load strongly predisposes to HAM/TSP. J. Neurovirol. 4 (6), 586–593.
Oh, U., Jacobson, S., 2008. Treatment of HTLV-I-associated myelopathy/tropical spastic paraparesis: toward rational targeted therapy. Neurol. Clin. 26, 781–797.
Osame, M, Usuku, K, Izumo, S, Ijichi, N, Amitani, H, Igata, A, Matsumoto, M, Tara, M., 1986. HTLV-I associated myelopathy, a new clinical entity. Lancet 1, 1031–1032.
Pinto, M.T., Rodrigues, E.S., Malta, T.M., Azevedo, R., Takayanagui, O.M., Valente, V.B., Ubiali, E.M., Covas, D.T., Kashima, S., 2012. HTLV-1/2 seroprevalence and coinfection rate in Brazilian first-time blood donors: an 11-year follow-up. Rev. Inst. Med. Trop. Sao Paulo 54, 123–129.
Ren, G., Zhang, L., Zhao, X., Xu, G., Zhang, Y., Roberts, A.I., Zhao, R.C., Shi, Y., 2008. Mesenchymal stem cell-mediated immunosuppression occurs via concerted action of chemokines and nitric oxide. Cell Stem Cell 2, 141–150.
Ren, G., Zhao, X., Zhang, L., Zhang, J., L'Huillier, A., Ling, W., Roberts, A.I., Le, A.D., Shi, S., Shao, C., Shi, Y., 2010. Inflammatory cytokine-induced intercellular adhesion molecule-1 and vascular cell adhesion molecule-1 in mesenchymal stem cells are critical for immunosuppression. J. Immunol. 184, 2321–2328.
Romieu-Mourez, R., François, M., Boivin, M.N., Stagg, J., Galipeau, J., 2007. Regulation of MHC class II expression and antigen processing in murine and human mesenchymal stromal cells by IFN-gamma, TGF-beta, and cell density. J. Immunol. 179, 1549–1558.
Scadden, D.T., Zeira, M., Woon, A., Wang, Z., Schieve, L., Ikeuchi, K., Lim, B., Groopman, J.E., 1990. Human immunodeficiency virus infection of human bone marrow stromal fibroblasts. Blood 76, 317–322.
Smirnov, S.V., Harbacheuski, R., Lewis-Antes, A., Zhu, H., Rameshwar, P., Kotenko, S. V., 2007. Bone-marrow-derived mesenchymal stem cells as a target for cytomegalovirus infection: implications for hematopoiesis, self-renewal and differentiation potential. Virology 360, 6–16.
Soderberg, C., Giugni, T.D., Zaia, J.A., Larsson, S., Wahlberg, J.M., Moller, E., 1993. CD13 (human aminopeptidase N) mediates human cytomegalovirus infection. J. Virol. 67, 6576–6585.
Stagg, J., Pommey, S., Eliopoulos, N., Galipeau, J., 2006. Interferon-gamma-stimulated marrow stromal cells: a new type of nonhematopoietic antigen-presenting cell. Blood 107, 2570–2577.
Starling, A.L., Martins-Filho, O.A., Lambertucci, J.R., Labanca, L., de Souza Pereira, S. R., Teixeira-Carvalho, A., Martins, M.L., Ribas, J.G., Carneiro-Proietti, A.B., Gonçalves, D.U., 2013. Proviral load and the balance of serum cytocines in HTLV-1-asymptomatic infection and in HTLV-1-associated myelopathy/tropical spastic paraparesis (HAM/TSP). Acta Trop. 125 (1), 75–81.
Sundin, M., Orvell, C., Rasmusson, I., Sundberg, B., Ringdén, O., Le Blanc, K., 2006. Mesenchymal stem cells are susceptible to human herpesviruses, but viral DNA cannot be detected in the healthy seropositive individual. Bone Marrow Transplant 37 (11), 1051–1059.
Tang, S.W., Chen, C.Y., Klase, Z., Zane, L., Jeang, K.T., 2013. The cellular autophagy pathway modulates human T-cell leukemia virus type 1 replication. J. Virol. 87 (3), 1699–1707.
Tendler, C.L., Greenberg, S.J., Burton, J.D., Danielpour, D., Kim, S.J., Blattner, W.A., Manns, A., Waldmann, T.A., 1991. Cytokine induction in HTLV-I associated myelopathy and adult T-cell leukemia: alternate molecular mechanisms underlying retroviral pathogenesis. J. Cell. Biochem. 46, 302–311.
Uchiyama, T., 1997. Human T cell leukemia virus type I (HTLV-I) and human diseases. Annu. Rev. Immunol. 15, 15–37.
Umehara, F., Izumo, S., Nakagawa, M., Ronquillo, A.T., Takahashi, K., Matsumuro, K., Sato, E., Osame, M., 1993. Immunocytochemical analysis of the cellular infiltrate in the spinal cord lesions in HTLV-I-associated myelopathy. J. Neuropathol. Exp. Neurol. 52, 424–430.
Umehara, F., Izumo, S., Ronquillo, A.T., Matsumuro, K., Sato, E., Osame, M., 1994. Cytokine expression in the spinal cord lesions in HTLV-I-associated myelopathy. J. Neuropathol. Exp. Neurol. 53, 72–77.
Wang, L., Mondal, D., La Russa, V.F., Agrawal, K.C., 2002. Suppression of clonogenic potential of human bone marrow mesenchymal stem cells by HIV type 1: putative role of HIV type 1 tat protein and inflammatory cytokines. AIDS Res. Hum. Retroviruses 18, 917–931.
Waterman, R.S., Tomchuck, S.L., Henkle, S.L., Betancourt, A.M., 2010. A new mesenchymal stem cell (MSC) paradigm: polarization into a pro-inflammatory MSC1 or an Immunosuppressive MSC2 phenotype. PLoS One 5, e10088.
Wei, G, Lin, M, Cai, Z, Huang, H., 2011. Cytomegalovirus infection in mesenchymal stem cells and their activation could be enhanced by nuclear factor-κB inhibitor pyrrolidinedithiocarbamate in vitro. Transplant Proc. 43, 1944–1949.
Yoshida, M., Seiki, M., Yamaguchi, K., Takatsuki, K., 1984. Monoclonal integration of human T-cell leukemia provirus in all primary tumors of adult T-cell leukemia suggests causative role of human T-cell leukemia virus in the disease. Proc. Natl. Acad. Sci. USA 81, 2534–2537.

AIDS RESEARCH AND HUMAN RETROVIRUSES
Volume 29, Number 00, 2014
© Mary Ann Liebert, Inc.
DOI: 10.1089/aid.2013.0036

Tax Posttranslational Modifications and Interaction with Calreticulin in MT-2 Cells and Human Peripheral Blood Mononuclear Cells of Human T Cell Lymphotropic Virus Type-I-Associated Myelopathy/Tropical Spastic Paraparesis Patients

Fernando Medina,[1,*] Sebastian Quintremil,[1,*] Carolina Alberti,[1] Andres Barriga,[1] Luis Cartier,[2] Javier Puente,[1] Eugenio Ramírez,[3] Arturo Ferreira,[4] Yuetsu Tanaka,[5] and Maria Antonieta Valenzuela[1]

Abstract

The human retrovirus human T cell lymphotropic virus type-I (HTLV-1) is the etiologic agent of HTLV-1-associated myelopathy/tropical spastic paraparesis (HAM/TSP). Axonal degeneration in HAM/TSP patients occurs without neuron infection, with the secreted viral Tax protein proposed to be involved. We previously found that Tax secreted into the culture medium of MT-2 cells (HTLV-1-infected cell line) produced neurite retraction in neuroblastoma cells differentiated to neuronal type. To assess the relevance of Tax posttranslational modifications on this effect, we addressed the question of whether Tax secreted by MT-2 cells and peripheral blood mononuclear cells (PBMCs) of HTLV-1-infected subjects is modified. The interaction of Tax with calreticulin (CRT) that modulates intracellular Tax localization and secretion has been described. We studied Tax localization and modifications in MT-2 cells and its interaction with CRT. Intracellular Tax in MT-2 cells was assessed by flow cytometry, corresponding mainly to a 71-kDa protein followed by western blot. This protein reported as a chimera with gp21 viral protein—confirmed by mass spectrometry—showed no ubiquitination or SUMOylation. The Tax–CRT interaction was determined by confocal microscopy and coimmunoprecipitation. Extracellular Tax from HAM/TSP PBMCs is ubiquitinated according to western blot, and its interaction with CRT was shown by coimmunoprecipitation. A positive correlation between Tax and CRT secretion was observed in HAM/TSP PBMCs and asymptomatic carriers. For both proteins inhibitors and activators of secretion showed secretion through the endoplasmic reticulum–Golgi complex. Tax, present in PBMC culture medium, produced neurite retraction in differentiated neuroblastoma cells. These results suggest that Tax, whether ubiquitinated or not, is active for neurite retraction.

Introduction

HUMAN T CELL LYMPHOTROPIC VIRUS TYPE-I (HTLV-1), the first human retrovirus discovered in the early 1980s, is the etiologic agent of two human pathologies: adult T cell leukemia (ATL) and HTLV-1-associated myelopathy/tropical spastic paraparesis (HAM/TSP).[1,2] HAM/TSP is a progressive neurological disease characterized by a central axonopathy, probably due to an axoplasmic transport disorder that produces a selective loss of long axons of corticospinal tracts.[3,4] Regarding infection, T-CD4$^+$ cells are the *in vivo* reservoir of the virus, mainly CD4$^+$FoxP3$^+$cells or T_{reg}.[5–7] Human cerebral endothelial cells have been shown to be susceptible to retroviral infection, producing a dysfunction of the blood–brain barrier by alteration in the expression of tight-junction proteins.[8] This could be an important

[1]Departamento de Bioquímica y Biología Molecular, Facultad de Ciencias Químicas y Farmacéuticas, Universidad de Chile, Santiago, Chile.
[2]Departamento de Ciencias Neurológicas, Facultad de Medicina, Universidad de Chile, Santiago, Chile.
[3]Programa de Virología, Facultad de Medicina, Universidad de Chile, and Departamento de Virología, ISP, Santiago, Chile.
[4]Programa de Inmunologia, ICBM, Facultad de Medicina, Universidad de Chile, Santiago, Chile.
[5]Department of Immunology, Graduate School and Faculty of Medicine, University of the Ryukyus, Nishihara, Japan.
*These authors contributed equally to this work.

mechanism for the infiltration of infected lymphocytes into the central nervous system (CNS) and also facilitates astrocyte infection.

Despite increasing knowledge about HTLV-1, the molecular mechanisms in HAM/TSP and the progression of the disease are still unknown since HTLV-1 does not infect *in vivo* neurons.[9] HAM/TSP has been associated with the expression and secretion of HTLV-1 Tax pleiotropic protein that exerts a role in viral and cellular transcription, cellular proliferation, and transformation.[4,10–16] Among the viral proteins, Tax is chronically detected in the cerebrospinal fluid of HAM/TSP patients.[17] Incubation of human SH-SY5Y neuroblastoma cells with culture medium of MT-2 cells (an HTLV-1-infected cell line that secretes viral Tax protein) produces neurite retraction and an increase in Tau phosphorylation at T181.[18]

Tax, a 40-kDa protein, undergoes posttranslational modifications such as phosphorylation, ubiquitination, SUMOylation, and acetylation.[15,16,19–24] Phosphorylation is critical for Tax transactivation via both the ATF/CREB and NF-κB pathways.[19,25] Ubiquitinated Tax is associated with cytoplasmic location, while SUMOylation is a nuclear retention signal of Tax resulting in NF-κB transcriptional activation.[20–24] Acetylation, predominantly in the nucleus, also facilitates NF-κB activation and positively correlates with Tax phosphorylation, being improved by previous SUMOylation.[15,25]

Recently, a critical role of K63-linked polyubiquitination of Tax has been shown at lysines K4 to K8 for Tax-induced NF-κB activation.[26,27] This modification is essential for Tax binding to NEMO/IKK-γ and IKK activation, while SUMOylation is dispensable. Tax nuclear import/export would occur through carrier- and energy-independent transport mechanisms; Tax may also have a carrier function.[12,28,29] Nevertheless, no Tax posttranslational modification studies have been performed in constitutively HTLV-1-infected lymphocytes (MT-2 cells) and in secreted products from HTLV-1 lymphocytes of infected individuals.

Alefantis *et al.*[30] reported that the calcium-binding protein calreticulin (CRT) interacts with Tax-GFP in BHK transfected cells, and the fluorescence signal was located near or at the nuclear membrane. They also observed in infected cells, including MT-2 cells, a higher expression of CRT compared with noninfected cell lines. Expression of Tax in Hep2 cells leads to a redistribution of CRT from the nucleus to the cytoplasm as shown by confocal microscopy with colocalization of Tax, CRT, NEMO/IKK-γ, and RelA in cytoplasmic dotted structures.[31]

Tax contains a number of putative secretory signals including YTNI and DHE, and interacts with cellular secretory pathway proteins in both a transfected cell line (BHK-21) and in an HTLV-1-infected cell line (C8166 cells, a human CD4$^+$ T lymphoblastoid cell line).[13] The secretion of Tax would occur by classical secretory pathways involving a vesicular transport mechanism through the endoplasmic reticulum (ER) and Golgi complex.[11,13,28]

The detection of Tax in cerebrospinal fluid of HAM/TSP patients and the neurite retraction produced by secreted products from MT-2 cells suggest that Tax could be a relevant protein in the pathogeny. In the present study, we followed Tax modifications with ubiquitin, SUMO-1, and SUMO-2/3 in MT-2 cells and in peripheral blood mononuclear cell (PBMC) culture medium from HTLV-1-infected subjects. In addition, CRT was determined in both types of samples to study Tax–CRT interaction/relationships and Tax posttranslational modifications related to HAM/TSP pathogenesis. Finally, we investigated whether Tax secreted from PBMCs of HAM/TSP patients also produced neurite retraction in neuroblastoma cells differentiated to neuronal type as Tax present in MT-2 cell culture medium.

Materials and Methods

Cell culture

Five to ten million MT-2 or K562 cells (control cell line) were cultured in 10 ml of RPMI 1640 + GlutaMAX (Invitrogen, Eugene, OR) supplemented with 10% fetal bovine serum (Invitrogen) as reported by Ramírez *et al.*[32]

HAM/TSP patients, asymptomatic HTLV-1 carriers, and healthy noninfected control subjects

All the experiments were performed in compliance with relevant laws and institutional guidelines and in accordance with the ethical standards of the Declaration of Helsinki. The University of Chile Ethics Committee has approved the research protocol and all individuals freely gave informed written consent. EDTA-treated blood was obtained from 14 HAM/TSP patients, three asymptomatic HTLV-1 carriers, and six healthy noninfected subjects (negative control).

PBMCs isolation and culture

PBMCs were isolated from 10 ml of EDTA-treated blood samples by Ficoll-Hypaque density gradient centrifugation and then were washed three times with phosphate-buffered saline (PBS; 137 mM NaCl, 2.7 mM KCl, 100 mM Na_2HPO_4, 2 mM KH_2PO_4, pH 7.2). We collected 2×10^6 PBMCs from each sample, which were cultured for 24 h in 1 ml of RPMI 1640 + GlutaMAX medium supplemented with 10% fetal bovine serum. The action of CD8$^+$ cytotoxic T lymphocytes was inhibited by 20 nM concanamycin A (Sigma-Aldrich, St Louis, MO) in order to express measurable Tax.[33] In Tax and CRT kinetics experiments from PBMCs, 1 μg/ml Brefeldin A (BFA) or 1 μg/ml ionomycin (IM) and 30 ng/ml phorbol myristate acetate (PMA) were added to the culture at 6 h. The cytotoxicity of BFA and IM + PMA treatments was assayed by measuring LDH release using the Pierce LDH Cytotoxicity Assay Kit, according to the manufacturer's instructions.

Flow cytometry

Cultured MT-2 cells (300,000) were harvested and washed twice with PBS and centrifuged at $400 \times g$ for 2 min. They were then stained with fluorophore-conjugated antibodies against CD4-FITC (dilution 1:25) (BD Biosciences, San Jose, CA) and Tax-APC (dilution 1:100) prepared in Dr. Yuetsu Tanaka's Laboratory. For Tax staining, cells were treated with 100 μl of fixation/permeabilization solution (eBiosciences, San Diego, CA) for 15 min at 4°C. Matched isotype controls were used at the same concentration as the respective antibodies. We performed two-color flow cytometry in a FACS-CANTO instrument (Beckton Dickinson); WinMDI 2.9 software was used for data analysis.

Immunocytochemistry and confocal microscopy

MT-2 and K562 cells were washed four times at 37°C with PBS. Cells were deposited on glass slides at a density of 10^4 cells per 10 μl, allowed to dry for 2–3 h at room temperature, fixed, and permeabilized in ice-cold acetone for 8 min. Fixed cells were incubated for 40 min at 37°C with 25 μl of both monoclonal anti-Tax (Covalab, diluted 1:50) and polyclonal anti-CRT (prepared in Dr. Arturo Ferreira's laboratory, diluted 1:200). After three washings with 250 μl PBS, cells were incubated in darkness for 40 min at 37°C with 25 μl of antimouse IgG secondary antibodies conjugated with FITC (Invitrogen, diluted 1:200) and antirabbit IgG conjugated with Alexa Fluor 594 (Invitrogen, diluted 1:400). The nuclear marker TO-PRO (Invitrogen) diluted 1:400 was also included. Cells were then washed three times with 250 μl of PBS and once with MilliQ water and led dried at room temperature. Coverslips were added with 2 μl of Gel mount Aqueous mounting medium (Sigma-Aldrich Inc.). The preparations were examined under a Carl Zeiss LSM 510 Meta confocal microscope. The images were obtained with LSM 510 Image Browser, and colocalization was analyzed with ImageJ, plugin Colocalization Finder software.

Cell lysis

Cells (MT-2, K562, or PBMCs) were washed five times with PBS and the last pellet was resuspended in lysis buffer (50 mM Tris–HCl, 150 mM NaCl, 1% Triton X-100, 0.5% Nonidet P-40, 10 mM *N*-ethylmaleimide, 0.2 mM Na_3VO_4, and 0.1 mM PMSF, pH 7.5). A total of 2×10^6 cells per 500 μl of lysis buffer was incubated on ice for 30 min with gentle shaking. Cell debris was pelleted by centrifugation at $16{,}000 \times g$ for 5 min at 4°C. The lysate was kept at −20°C. Subcellular fractionation of MT-2 cells was performed according to Kfoury *et al.*[23] to obtain three different fractions enriched in cytoplasmic, intermediate fraction (organellar membrane), and nuclear components.

Protein determination, SDS-PAGE, and western blot analysis

Protein determination of cell lysate was done using the Micro BCA Protein Assay Kit from Pierce (Pierce Biotechnology Inc., Rockford, IL) according to the manufacturer's instructions. SDS–PAGE under reducing conditions was performed with 10% polyacrylamide gels. Portions of 50 μg protein of cell lysate or 20 μl of PBMC culture medium were used. The buffer for electrotransfer to nitrocellulose membranes (Bio-Rad Laboratories Ltd., Hercules, CA) contained 25 mM Tris–HCl, 192 mM glycine, and 20% methanol, and electrotransfer was done at a total current of 600 mA at 4°C. After electrotransfer, membranes were blocked for 20 min at room temperature with 5% p/v of "Quick blocker" (Chemicon International, Temecula, CA) dissolved in TBS-T (20 mM Tris–HCl, 137 mM NaCl, 0.1% Tween-20, pH 7.6), then incubated overnight at 4°C or 2 h at room temperature with different primary antibodies at the appropriate dilution in TBS-T buffer.

The following monoclonal antibodies were used: two anti-Tax antibodies (Covalab. Cat. mab0022, diluted 1:1,000) and HTLV-1 Tax hybridoma 168A51-2 (NIH, AIDS Reagent Program, Germantown, MD; Cat. 1316, used as ascitic fluid, diluted 1:1,000), antibodies against ubiquitin (Upstate, Lake Placid, NY; Cat. 04-263, diluted 1:1,000), SUMO-1 (Upstate; Cat. 04-453, diluted 1:1,000), SUMO-2/3 (Abcam Inc., Cambridge, MA; Cat. Ab3742, diluted 1:1,000), GAPDH (Sigma-Aldrich Inc.; Cat. G8795, diluted 1:20,000), TFIIB (Santa Cruz Biotechnology Inc., Santa Cruz, CA; Cat. sc-225, diluted 1:1,000), Dynein IC1/2, cytosolic (Santa Cruz Biotechnology Inc.; Cat. sc-13524, diluted 1:500), MMP-9 (Millipore Merck, Billerica, MA; Cat. MAB3309, diluted 1:500), and polyclonal antibodies against CRT prepared in Dr. Arturo Ferreira's laboratory (diluted 1:5,000 or 1:800,000 according to the antibody titer). After washing five times (5 min each wash) with TBS-T, membranes were incubated with the appropriate secondary antibody for 1 h at room temperature.

As secondary antibodies the following were used: ImmunoPure Goat Anti-Rabbit IgG (H+L) Peroxidase Conjugated (Pierce, diluted 1:500,000), ImmunoPure Goat Anti-Mouse IgG (H+L) Peroxidase Conjugated (Pierce, diluted 1:500,000), and Donkey Anti-Mouse antibody, HRP conjugated, diluted 1:250 (SA1100, Thermo Fisher Scientific, Rockford, IL; absorbed against the sera of several animal species). After washing five times (5 min each wash) with TBS-T the reaction product was visualized using enhanced chemiluminescence SuperSignal West Femto Maximum Sensitivity Substrate Chemiluminescent substrate (Pierce). X-Ray films (CL-Xposure film, Pierce) were exposed for varying times. Control experiments without primary antibodies (only with secondary antibodies) did not give any chemiluminescent signal. For consecutive analyses with various antibodies, stripping was performed, rinsing twice for 10 min with 200 mM glycine, 3.5 mM SDS, and 10% Tween-20 at pH 2.2. Blots were then blocked and probed as described above. Quantification of blots was carried out by scanning films using the Uni-Scan-It Automated Digitizing System.

Coimmunoprecipitation studies

Portions of 500 μg of protein from cell lysates or 500 μl of PBMC culture medium were captured with either anti-Tax (Covalab), anti-CRT, anti-Dynein, or anti-MMP-9 antibodies bound to the coupling resin of the "AminoLink Plus Immobilization Kit" (Pierce). Tax and CRT antibody binding, sample application, and protein elution were done according to the manufacturer's instructions. Proteins eluted from the matrix were subjected to SDS–PAGE and/or western blot.

Mass spectrometry analysis

Excised protein bands (stained with GelCode Blue Stain Reagent, Bio-Rad) were destained, DTT and iodoacetamide treated, and proteolyzed with Trypsin. Peptides from proteolysis and extraction were concentrated using SpeedVac. Concentrated peptides were redissolved in 10 μl of 0.1% formic acid for MALDI-TOF analysis or in 30 μl of 0.1% formic acid and 5% methanol for LC-MS/MS analysis. For MALDI-TOF analysis, the dissolved peptides were mixed with CHCA matrix (10 mg/ml) in a 1:1 ratio. Spectra were acquired in a Microflex MALDI-TOF instrument (Bruker Daltonics Inc., Billerica, MA). Mass list was analyzed in Mascot, MS-Fit, and ProFound on-line databases. Additionally, experimental data were examined using the PeptideMap tool from PROWL against the Tax sequence. For LC-MS/MS analysis 20 μl of the dissolved peptides was

separated on a C_{18} column (Jupiter-Proteo 150×1.0 mm, 4 μm, and 90 Å, Phenomenex Inc., Torrance, CA) at room temperature using the following conditions: 0–10 min 2% B, 10–70 min 2–100% B, and 70–80 min 100% B, where mobile phase A was 0.1% formic acid in water and mobile phase B was 0.085% formic acid in 80% acetonitrile. Chromatograms and spectra were recorded at positive mode on an Esquire 4000 LC-ESI IT MS/MS instrument (Bruker Daltonik GmbH, Germany). Experimental data were examined on the Mascot on-line database and on the local Mascot server against Tax (GenBank accession number BAB18052) and Env protein (GenBank accession number AAU04944) sequences.

Neurite retraction studies on SH-SY5Y cells

Neuroblastoma cells were differentiated with 10 μM *all-trans*-retinoic acid (Sigma-Aldrich) and 50 ng/ml of BDNF (Alomone Laboratories, Jerusalem, Israel).[18] BDNF was removed from the culture medium and replaced by a mixture of DMEM-F12 Ham without fetal bovine serum 4 h previous to the addition of culture medium of PBMCs. In all experiments DMEM-F12 was replaced by PBMC culture medium, being differentiated in SH-SY5Y cells incubated up to 2 h with (1) culture medium of PBMCs from an HAM/TSP patient, (2) culture medium of PBMCs from an HAM/TSP patient with 10 μl/ml of either Tax antibody (HTLV-1 Tax Hyb 168A51-2) or a same isotype irrelevant antibody (anti-Gizzerosine), and (3) with culture medium of PBMCs from a healthy subject. Neurite retraction was followed measuring neurite length using the NIH ImageJ-1.38d program plug in NeuronJ according to Maldonado *et al.*[18] Data collected from 200–300 neurites were used for each condition. All experiments were done in triplicate. Neurite length was expressed as the average value of (μm)/cell ± SEM.

Statistical analysis

Statistical data analysis was performed using GraphPad Prism 5.0 and SPSS (version 13, SPSS Inc., Chicago, IL). Data were verified for Gaussian distribution using the Shapiro Wilk test. Spearman's correlation coefficient was used to evaluate relationships between Tax and CRT protein levels.

Results

Tax expression, localization, and modifications in MT-2 cells

MT-2 cells are widely used as a lymphoid line in HTLV-1 research because they contain HTLV-1 in their genome as a provirus. About 50% of these cells express Tax followed by flow cytometry as is shown in Fig. 1A. Cell fractionation yielded fractions enriched in (1) cytosolic proteins, (2) cell membrane and organelle proteins (intermediate fraction), and (3) nuclear proteins.[23] Tax in western blot analysis corresponds mainly to a 71-kDa protein as shown in Fig. 1B. This band is observed only in the intermediate fraction. To evaluate the presence of modifications, antibodies against ubiquitin, SUMO-1, and SUMO-2/3 were used in western blot analysis. However, neither of them was found to be associated with the 71-kDa band (data not shown). Additionally, Tax immunoprecipitation did not enable detection of these posttranslational modifications.

According to the literature, Tax could be fused with Env or Gag proteins in MT-2 cells as a consequence of chromosomal aberration.[34,35] Glycosylated Env is an immature protein that undergoes a proteolytic processing giving rise to two glycosylated membrane proteins, gp46 and gp21. Therefore, the C-terminal end of gp21 could be fused with translated Tax (Env-Tax). Tax was submitted to immunoprecipitation, Trypsin digestion, and MALDI-TOF/ESI-IT mass spectrometry analysis. The sequences of two Tax peptides (41-HALLATCPEHQITWDPIDGR-60 and 87-VLTPPITHTTP NIPPSFLQAMR-108) and two gp21 peptides (441-EALQ TGITLVALLLLVILAGPCILR-465 and 469-HLPSRVRY PHYSLINPESSL-488) were found. These results are in agreement with the previously described fusion protein between gp21 and Tax present in MT-2 cells, accounting for the difference in electrophoretic migration, discarding ubiquitin-like posttranslational modifications.

Tax, upon 2-fold concentration from MT-2 culture medium, was found only as a 40-kDa nonmodified form by western blot (unpublished results). The 71-kDa membrane-associated form was not found as expected, because it is not a secretable protein.

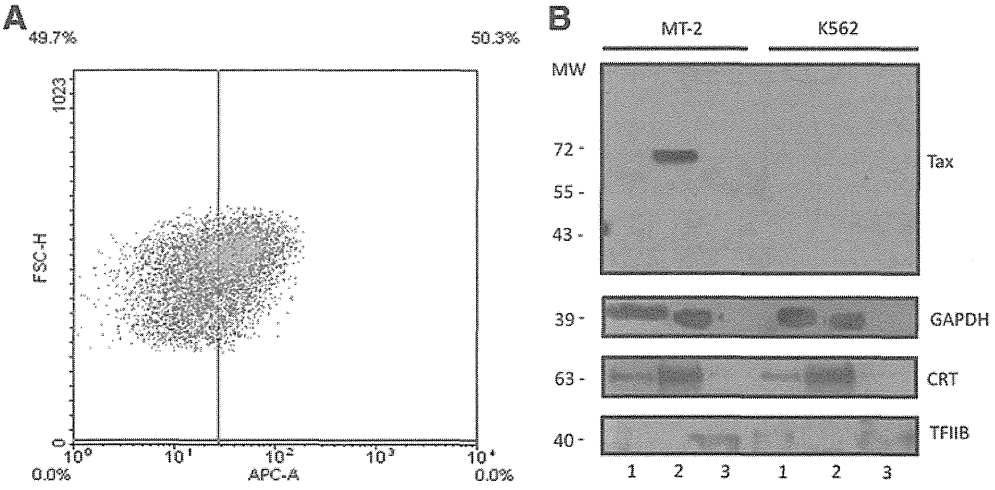

FIG. 1. Tax expression in MT-2 cells. **(A)** Flow cytometry analysis of MT-2 cell culture, showing about 50% of Tax expressing cells (anti-Tax APC diluted 1:100). **(B)** Western blot of MT-2 or K562 cell fractionation into cytosolic (lanes 1), intermediate (lanes 2), and nuclear (lanes 3) fractions. The figure shows western blots using antibodies against Tax (Covalab, diluted 1:1,000), GAPDH (cytosolic marker, diluted 1:20,000), calreticulin (CRT) ER marker, diluted 1:5,000), and TFIIB (nuclear marker, diluted 1:1,000).

Tax and CRT interaction in MT-2 cells

According to the literature, Tax is a secretable protein in *tax*-transfected cells and CRT seems to be involved in the Tax nuclear export into the cytoplasm.[12,30] Consequently, CRT could participate in Tax intracellular localization, including secretion mechanisms. The interaction between Tax and CRT was determined by immunofluorescence colocalization and coimmunoprecipitation in MT-2 cells. According to confocal microscopy among a total of 500 observed cells, 57% expressed Tax protein, which agrees with previous flow cytometry data analysis (Fig. 1A). A total of 42% of Tax expressing cells showed CRT colocalization (Fig. 2A). The interaction between these proteins was confirmed by coimmunoprecipitation with either anti-Tax or anti-CRT antibodies (Fig. 2B). None of the immunoprecipitated complexes showed the presence of other irrelevant proteins (SUMO-1, SUMO-2/3, and ubiquitin). Immunoprecipitation using an irrelevant antibody (Dynein) as a negative control demonstrated the absence of Env-Tax and CRT (Fig. 2B), pointing to a specific interaction of Tax and CRT that could be involved in the secretion pattern of Tax in HTLV-1-infected cells.

Tax expression in cultured PBMCs from infected subjects

After 24 h culture, PBMCs from HTLV-1-infected patients expressed Tax protein at detectable levels by flow cytometry,[7] but not by western blot. Nevertheless, secreted Tax can be followed by western blot in PBMC culture medium, which indicates Tax secretion. We did not find a significant correlation between Tax content in HAM/TSP patients and disease progression. Posttranslational modifications determined in secreted Tax from infected PBMCs by western blot of the culture medium from a set of different HAM/TSP patients and asymptomatic HTLV-1 carriers showed an immunoreactive band for Tax that matches that for ubiquitin (Fig. 3A). Tax ubiquitination was confirmed after immunoprecipitation with anti-Tax antibodies, while modifications with SUMO-1 or SUMO-2/3 were not detected in that immunoprecipitate, which agrees with a secreted protein form (Fig. 3B). Since ubiquitin's molecular weight is about 8.5 kDa, the 57-kDa form might correspond to Tax modification with two ubiquitin subunits. Differences observed in Tax electrophoretic migration in Fig. 3B are caused by serum proteins in PBMC culture medium that are absent in the immunoprecipitated sample.

Tax and CRT secretion in PBMCs of HAM/TSP patients

CRT was found in the PBMC culture medium of HAM/TSP patients as a broad band (ranging from 87 to 70 kDa) and a discrete band at 56 kDa (Fig. 4A). To understand the secretion mechanisms of CRT and Tax protein, PBMCs of three patients were incubated with either Brefeldin A or with ionomycin (IM) and phorbol myristate acetate (PMA). The former inhibits protein transport from the ER to the Golgi; the

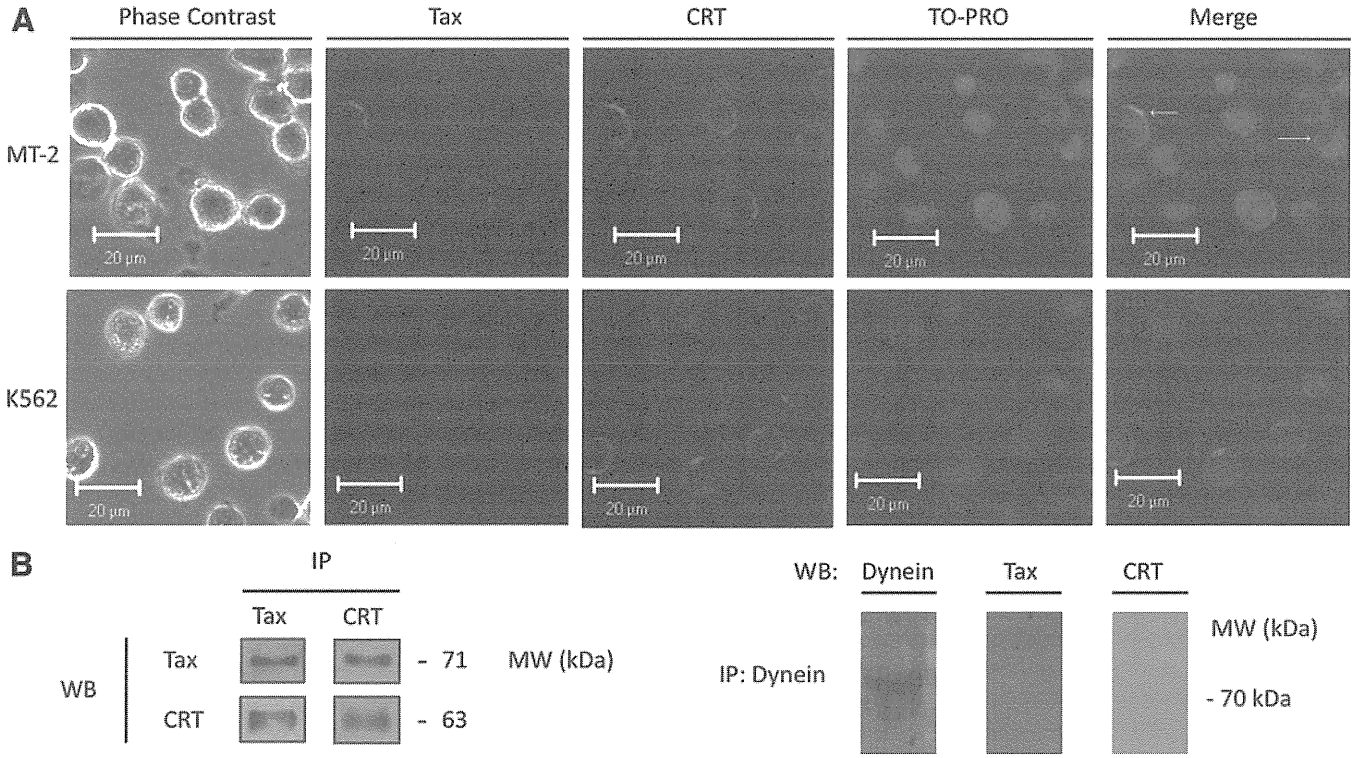

FIG. 2. Tax and CRT interaction in MT-2 cells. **(A)** Indirect immunofluorescence of Tax (anti-Tax Covalab diluted 1:50; secondary antibody FITC labeled, green) and CRT (anti-CRT diluted 1:200; secondary antibody Alexa Fluor 594 labeled, red)-stained MT-2 and K562 cells by confocal microscopy. Nuclei were labeled with TO-PRO (blue pseudocolor). White arrows indicate colocalization points of Tax and CRT. **(B)** Coimmunoprecipitation of Env-Tax and CRT from whole cells lysate of MT-2 cells. Tax and CRT were detected by western blot (WB) in both, Tax and CRT immunoprecipitated (IP), using anti-Tax NIH diluted 1:1,000 and anti-CRT diluted 1:5,000. As control, immunoprecipitation with anti-Dynein was performed. Dynein was detected by western blot using anti-Dynein diluted 1:500.

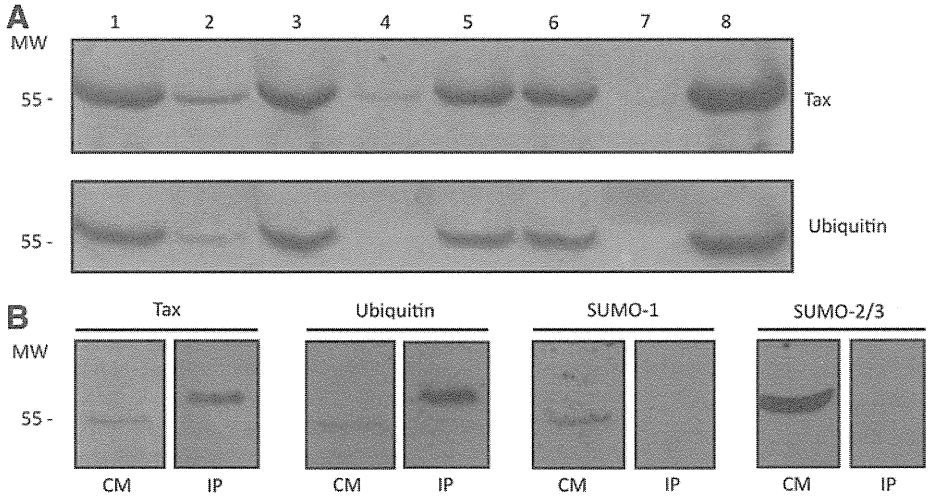

FIG. 3. Tax posttranslational modifications in peripheral blood mononuclear cell (PBMC) culture medium from HTLV-1-associated myelopathy/tropical spastic paraparesis (HAM/TSP) patients. (**A**) Representative western blot for Tax identification (using antibodies against Tax, Covalab diluted 1:1,000) and ubiquitin modification in PBMC culture medium of HAM/TSP patients (lanes 1, 2, 4, 5, and 8), asymptomatic carriers (lanes 3 and 6), and healthy noninfected control (lane 7) determined by western blot. (**B**) Tax immunoprecipitation (IP) from PBMC culture medium (CM) and identification of Tax (using antibodies against Tax, NIH diluted 1:1,000), ubiquitin (diluted 1:1,000), SUMO-1 (diluted 1:1,000), and SUMO-2/3 (diluted 1:1,000) by western blot.

latter—IM and PMA—increase protein secretion. Cytotoxicity assays measured as LDH release, expressed as mean value ± SD, showed the following values: for BFA treatment 0.210 ± 0.012, for IM + PMA treatment 0.176 ± 0.085, and for the control condition 0.237 ± 0.023 after 12 h culture. No significant differences among the three conditions were found. The results obtained agree with a canonical secretion mechanism for both proteins in HTLV-1-infected PBMCs: Brefeldin A reduced the secretion of both Tax and CRT proteins, while IM and PMA increased their secretion levels (Fig. 4B).

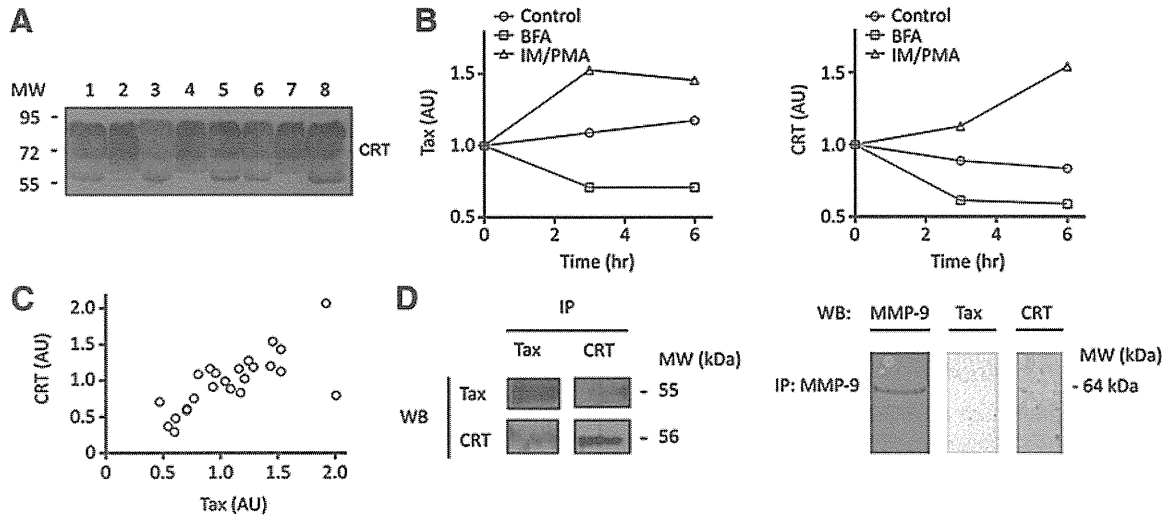

FIG. 4. Tax and CRT secretion from PBMCs of HAM/TSP patients. (**A**) Representative western blot for CRT secreted from PBMC samples of HAM/TSP patients (lanes 1, 2, 4, 5, and 8), asymptomatic carriers (lanes 3 and 6), and healthy noninfected control (lane 7) determined in PBMC culture medium by western blot (anti-CRT, diluted 1:5,000). (**B**) Tax and CRT kinetics release from PBMCs of a representative HAM/TSP patient. Cells were cultured in control condition (Control) and determinations were made after 16 h of PBMC culture in the presence of Brefeldin A (BFA) or ionomycin/PMA (IM/PMA). Proteins were determined by western blot during 24 h of culture (anti-Tax NIH diluted 1:1,000 using as secondary antibody a donkey antimouse 1:250 absorbed against the sera of several animal species; anti-CRT diluted 1:800,000). Data are expressed in arbitrary units (AU) of pixel intensity corresponding to Tax and CRT normalized with respect to the initial value. (**C**) Direct relationship between Tax and 56-kDa CRT (AU) released levels from PBMC culture medium of HAM/TSP patients shown in (**B**). A significant positive correlation of 0.766 was found according to Spearman's correlation ($p < 0.05$, 24 data of XY pairs). (**D**) Coimmunoprecipitation of Tax and CRT from PBMC culture medium. Tax and CRT were detected by western blot (WB) in both Tax and CRT immunoprecipitations (IP). As control, immunoprecipitation with anti-MMP-9 was performed. MMP-9 was detected by western blot using anti-MMP-9 diluted 1:500.

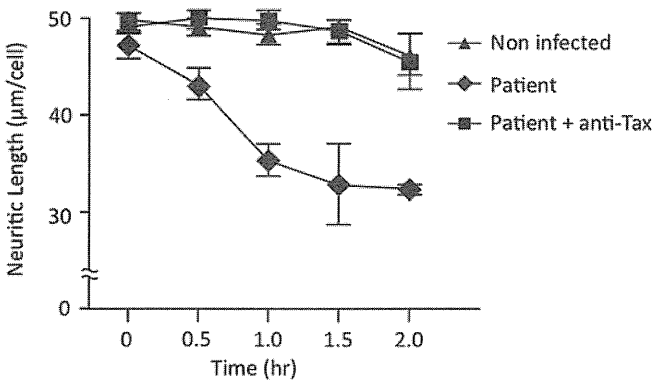

FIG. 5. Effect of PBMC culture medium on SH-SY5Y neurite length. Neurite length, expressed as (μm/cell ± SEM collected from 200–300 neurites for each condition, was measured using the NIH ImageJ-1.38d program plug in neuronJ. Differentiated SH-SY5Y cells were incubated with PBMC culture medium of a noninfected subject (healthy subject), of an HAM/TSP patient, and the same culture of the HAM/TSP patient including anti-Tax (HTLV-1 Tax Hyb 168A51-2). After 30 min of treatment, significant differences between the HAM/TSP sample and the two control conditions were found ($p < 0.05$).

A positive correlation (Spearman's correlation coefficient of 0.8) between Tax protein and the 56-kDa band of CRT was found in PBMC culture medium of 14 HAM/TSP patients and three HTLV-1 carriers studied (data not shown). A similar positive correlation was determined between Tax and CRT during the time course of secretion of PBMCs cultured with Brefeldin A or IM/PMA for the three patients under study (Fig. 4C). Immunoprecipitation with either anti-Tax or anti-CRT antibodies from PBMC culture medium indicated coprecipitation of Tax and CRT (Fig. 4D). Immunoprecipitated complexes did not show other irrelevant proteins such as SUMO-1 and SUMO-2/3. Immunoprecipitation with an irrelevant antibody (MMP-9, secretable protein), used as negative control, evidenced the absence of Tax and CRT (Fig. 4D), confirming the specific interaction between these proteins. All these results suggest a common vesicular transport for secretion of both proteins.

Effect of secreted Tax from human PBMCs on neurite retraction of SH-SY5Y cells

Figure 5 shows the effect of PBMC culture medium of an HAM/TSP patient on differentiated neuroblastoma cells, SH-SY5Y cells, using as control the culture medium of a healthy subject. Neurite retraction (neurite shortening) was observed with secreted medium from PBMCs of the HAM/TSP patient. Inclusion of anti-Tax antibody prevented the retraction effect. The presence of an irrelevant antibody did not modify the neurite shortening produced by PBMC culture medium of the HAM/TSP patient (data not shown).

Discussion

Tax regulation and interaction with cellular proteins and transcriptional complexes in HTLV-1-infected cells are widely accepted as essential factors in virus replication and disease progression.[14] Posttranslational modifications of Tax modulate its transcriptional activities and intracellular localization.[36] Tax protein has been detected in the nucleus and in three extranuclear compartments: around the microtubule organizer center, colocalizing with the centrosome and associated with the Golgi complex, and also in the region of the virological synapse.[23,37] Tax localization in both the nucleus and cytoplasm is important for activation of the NF-κB pathway.[24] The canonical NF-κB pathway requires NEMO/IKK-γ, which acts as a platform for recruitment of activators and inhibitors of the IKK complex (effector subunits IKK-α and IKK-β).[24] K63-linked polyubiquitination at lysines K4 to K8 of Tax promotes the targeting of Tax and NEMO to perinuclear spots associated with the Golgi complex. After their interaction with IKK-α and IKK-β, nuclear translocation of RelA occurs.[24,26,27]

In HAM/TSP patients, the mechanisms related to extracellular Tax on disease occurrence and progression remain to be elucidated. In this pathology, the extracellular Tax action has been considered relevant mostly because of the following evidence: (1) about 40% of patients with paraparesis are seronegative for HTLV-1 but exhibit a truncated virus form with the Tax gene incorporated[10] and (2) the neurite shortening (retraction) effect of secreted Tax from culture medium of MT-2 cells on differentiated human neuroblastoma cells.[18] In this *in vitro* model of the disease, we also found an increase in CdK5 activity that could be involved in extracellular Tax signaling. The participation of this viral protein was confirmed by the blocking effect of anti-Tax antibodies.[18]

Cell-free Tax detected in cerebrospinal fluid of HAM/TSP patients comes from secretion of infected cells, mainly $CD4^+$ T cells.[17] Increasing evidence suggests an extracellular axonal effect of Tax protein related to the occurrence and progression of HAM/TSP.[13,18,30,38] Infected lymphocytes are initially in the CNS regions including periventricular areas of the blood–brain barrier, the subarachnoid space, and the thoraxic and lumbar region.[39] Brain endothelial cells that express the receptors for HTLV-1 (GLUT-1, Neuropilin-1, and HSPG) can be infected, producing a dysfunction of the brain–blood barrier, increasing its permeability, thus facilitating lymphocyte passage through the endothelial monolayer cells.[8]

We identified ubiquitinated Tax protein in the culture medium of PBMCs isolated from HTLV-1 carriers and HAM/TSP patients (Fig. 3). Isolated Tax showed the presence of at least two ubiquitin units deduced from a molecular weight of 57 kDa. This modification should correspond to K63-linked ubiquitination since K48-linked ubiquitination is related to proteasomal degradation.[40] The lack of SUMO groups corroborated that Tax corresponds to a secreted protein form since this modification is considered a nuclear retention signal.[21,22] To our knowledge, this is the first evidence of ubiquitinated Tax secretion from infected lymphocytes of HAM/TSP patients and HTLV-1 carriers. Furthermore, CRT levels in culture medium are associated with Tax extracellular levels, which would point to a common secretion mechanism as shown in Fig. 4.

CRT, a classical ER resident protein, could participate in the destination of Tax protein to the canonical secretory pathway.[30] This can be explained by at least two putative secretory signals in Tax, allowing the secretion of both Tax and CRT as we have observed.[11,13] In the current study, CRT secretion in culture medium of PBMCs supports the growing evidence that CRT is not confined in the ER as initially

described by Michalak in 1992.[41,42] CRT has been found in cytoplasm, nucleus, Golgi, plasma membrane, and even extracellularly in many cell types and tissues, despite of the C-terminal ER localization signal (KDEL) and the lack of secretory signals.[41,42] In Hep2 cells, Tax leads to a redistribution of CRT from the nucleus to the cytoplasm.[31] Some authors suggest a cleavage of the ER retention signal or interaction with another protein masking the KDEL sequence.[41] Tax interaction with CRT in HTLV-1-infected lymphocytes might be involved in ER retention signal masking. Moreover, Tax interaction with various proteins might form complexes involved in the regulated secretion pathway. Tax could act as a carrier protein for CRT trafficking via secretion vesicles in HTLV-1-infected lymphocytes.[13] Thus, Tax and CRT could be cosecreted, which would imply a new mechanism of CRT and Tax secretion. Our results show a positive correlation between Tax and the 56-kDa CRT levels in PBMC culture medium of HAM/TSP patients and also coincide with the similar secretion of both proteins.

CRT is widely accepted as a multifunctional protein and current information describes some extracellular effects of CRT, such as promoting wound healing, cell survival, and participating in immune responses against cancer cells.[41,42,43] Thus, CRT in extracellular environments favors human health. HTLV-1 has evolved along with humans since ancient times and has a variety of immunological escape and host survival mechanisms.[44,45] Consequently, the higher levels of secreted CRT would have beneficial effects on HTLV-1-infected subjects, providing survival mechanisms that would counteract the deleterious effects of Tax.

Our studies on Tax posttranslational modifications in the HTLV-1-infected MT-2 cell line discard the modifications with ubiquitin-like proteins; however, Tax was detected as a fusion protein with gp21—a membrane HTLV-1 glycoprotein.[34,35,46] Previous studies showed an interaction between Tax and CRT near the nuclear membrane of the BHK-21 cell line cotransfected with *tax* and *crt* genes.[30] These authors identified CRT as a nuclear export receptor for Tax, suggesting a control checkpoint for nuclear export, including an additional complexity level to the Tax intracellular location. We found this interaction in MT-2 cells of the cytoplasmic region, probably in ER structures where CRT preferentially locates and interacts with different proteins during folding and quality control of secreted proteins.[47] In these infected cells, we demonstrated that the Tax–CRT interaction occurred by immune colocalization and coimmunoprecipitation, similar to that reported in transfected cells with both *tax* and *crt* genes.[30]

The steady state of K63-linked ubiquitination of Tax seems to depend on Ubc13, an E2 ubiquitin-conjugating enzyme, while the ubiquitin-specific peptidase USP20 would act as a ubiquitin-editing enzyme.[24,26,48,49] On the other hand, this peptidase was detected in Tax transfected HEK293T cells, with reduced activity, as well as in several HTLV-1 transformed cells such as MT-1, MT-2, MT-4, and AT-2.[48] We detected a ubiquitinated Tax form only in infected human PBMCs, probably indicating that peptidase might be less active or absent in these cells.

In conclusion, our study reveals differences between the Tax secreted from HTLV-1-infected T-lymphocytes—which becomes ubiquitinated—and that from MT-2 cells. Tax secretion occurs via the classical ER–Golgi pathway, where CRT may be involved in a cosecretion mechanism due to the extracellular interaction of Tax and CRT. The similar effects of the 40-kDa Tax present in supernatants of MT-2 cells[18] and the 57-kDa Tax form in HAM/TSP PBMC supernatants indicate the ubiquitin-independent neurotoxic effect of this secretable viral protein.

Sequence Data

Accession numbers: HTLV-1 Tax, BAB18052; HTLV-1 envelope glycoprotein, AAU04944.

Acknowledgments

We thank Professor Claudio Telha for his valuable input when reviewing the manuscript. We are grateful to Fondecyt, which supported this study (Grant Fondecyt 108-0396), to Project Mecesup UCH 0115, which allowed the use of the Mass Spectrometry Instrument, to the doctoral thesis supported by CONICYT no. 24090150, and to the master thesis supported by CONICYT no. 22110639. We also thank the NIH AIDS Reagent Program for the HTLV-1 Tax hybridoma.

Author Disclosure Statement

No competing financial interests exist.

References

1. Poiesz BJ, Ruscetti FW, Gazdar AF, Bunn PA, Minna JD, and Gallo RC: Detection and isolation of type C retrovirus particles from fresh and cultured lymphocytes of a patient with cutaneous T-cell lymphoma. Proc Natl Acad Sci USA 1980;77:7415–7419.
2. Yoshida M, Miyoshi I, and Hinuma Y: Isolation and characterization of retrovirus from cell lines of human adult T-cell leukemia and its implication in the disease. Proc Natl Acad Sci USA 1982;79:2031–2035.
3. Cartier L, Cea JG, Vergara C, Araya F, and Born P: Clinical and neuropathological study of six patients with spastic paraparesis associated with HTLV-1: An axomyelinic degeneration of the central nervous system. J Neuropathol Exp Neurol 1997;56:403–413.
4. Cartier L, Vergara C, and Valenzuela MA: Immunohistochemistry of degenerative changes in the central nervous system in spastic paraparesis associated to human T lymphotropic virus type I (HTLV-1). Rev Med Chil 2007;135:1139–1146.
5. Yamano Y, Takenouchi N, Li H, Tomaru U, Yao K, Grant C, Maric D, and Jacobson S: Virus-induces dysfunction of CD4+CD25+ T cells in patients with HTLV-1-associated neuroimmunological disease. J Clin Invest 2005;115:1361–1368.
6. Toulza F, Heaps A, Tanaka Y, Taylor GP, and Bangham CR: High frequency of CD4+Foxp3+ cells in HTLV-1 infection: Inverse correlation with HTLV-1-specific CTL response. Blood 2008;111:5047–5053.
7. Alberti C, Cartier L, Valenzuela MA, Puente J, Tanaka Y, and Ramirez E: Molecular and clinical effects of betamethasone in human T-cell lymphotropic virus type-1-associated myelopathy/tropical spastic paraparesis patients. J Med Virol 2011;83:1641–1649.

8. Afonso PV, Ozden S, Cumont MC, *et al.:* Alteration of blood–brain barrier integrity by retroviral infection. PLoS Pathog 2008;4:e1000205.
9. Grant C, Barmak K, Alefantis T, Yao J, Jacobson S, and Wigdahl B: Human T cell leukemia virus type I and neurologic disease: Events in bone marrow, peripheral blood, and central nervous system during normal immune surveillance and neuroinflammation. Cell Physiol 2002;190: 133–159.
10. Ramírez E, Fernández J, Cartier L, Villota C, and Ríos M: Defective human T-cell lymphotropic virus type I (HTLV-1) provirus in seronegative tropical spastic paraparesis/ HTLV-1-associated myelopathy (TSP/HAM) patients. Virus Res 2003;91:231–239.
11. Alefantis T, Mostoller K, Jain P, Harhaj E, Grant C, and Wigdahl B: Secretion of the human T cell leukemia virus type I transactivator protein tax. J Biol Chem 2005;280: 17353–17362.
12. Alefantis T, Jain P, Ahuja J, Mostoller K, and Wigdahl B: HTLV-1 Tax nucleocytoplasmic shuttling, interaction with the secretory pathway, extracellular signaling, and implications for neurologic disease. J Biomed Sci 2005;12:961–974.
13. Jain P, Mostoller K, Flaig KE, *et al.:* Identification of human T cell leukemia virus type 1 tax amino acid signals and cellular factors involved in secretion of the viral oncoprotein. J Biol Chem 2007;282:34581–34593.
14. Boxus M, Twizere JC, Legros S, Dewulf JF, Kettmann R, and Willems L: The HTLV-1 Tax interactome. Retrovirology 2008;5:76.
15. Lodewick J, Lamsoul I, Polania A, *et al.:* Acetylation of the human T-cell leukemia virus type 1 Tax oncoprotein by p300 promotes activation of the NF-kappaB pathway. Virology 2009;386:68–78.
16. Lodewick J, Lamsoul I, and Bex F: Move or die: The fate of the Tax oncoprotein of HTLV-1. Viruses 2011;3:829–857.
17. Cartier L and Ramírez E: Presence of HTLV-1 Tax protein in cerebrospinal fluid from HAM/TSP patients. Arch Virol 2005;150:743–753.
18. Maldonado H, Ramirez E, Utreras E, *et al.:* Inhibition of cyclin-dependent kinase 5 but not of glycogen synthase kinase 3-β prevents neurite retraction and tau hyperphosphorylation caused by secretable products of human T-cell leukemia virus type I-infected lymphocytes. J Neurosci Res 2011;89:1489–1498.
19. Durkin S, Ward M, Fryrear K, and Semmes O: Site-specific phosphorylation differentiates active from inactive forms of the human T-cell leukemia virus type 1 Tax oncoprotein. J Biol Chem 2006;281:31705–31712.
20. Peloponese JM Jr, Iha H, Yedavalli VR, *et al.:* Ubiquination of human T-cell leukemia virus type 1 Tax modulates its activity. J Virol 2004;78:11686–11695.
21. Lamsoul I, Lodewick J, Lebrun S, *et al.:* Exclusive ubiquination and SUMOylation on overlapping lysine residues mediate NF-kB activation by the human T-cell leukemia virus Tax oncoprotein. Mol Cell Biol 2005;25:10391–10406.
22. Nasr R, Chiari E, El-Sabban M, *et al.:* Tax ubiquitination and SUMOylation control critical cytoplasmic and nuclear steps of NF-kB activation. Blood 2006;107:4021–4029.
23. Kfoury Y, Nasr R, Favre-Bonvin A, *et al.:* Ubiquitylated Tax targets and binds the IKK signalosome at the centrosome. Oncogene 2008;27:1665–1676.
24. Kfoury Y, Nasr R, Journo C, Mahieux R, Pique C, and Bazarbachi A: The multifaceted oncoprotein Tax: Subcellular localization, posttranslational modifications, and NF-kB activation. Adv Cancer Res 2012;113:85–120.
25. Jeang KT: Functional activities of the human T-cell leukemia virus type I Tax oncoprotein: Cellular signaling through NF-kappa B. Cytokine Growth Factor Rev 2001; 12:207–217.
26. Journo C, Bonnet A, Favre-Bonvin A, *et al.:* HTLV-2 Tax-mediated NF-κB activation involves a mechanism independent of Tax conjugation to ubiquitin and SUMO. J Virol 2013;87:1123–1136.
27. Bonnet A, Randrianarison-Huetz V, Nzounza P, *et al.:* Low nuclear body formation and tax SUMOylation do not prevent NF-kappaB promoter activation. Retrovirology 2012; 9:77.
28. Alefantis T, Barmak K, Harhaj EW, Grant C, and Wigdahl B: Characterization of a nuclear export signal within the human T cell leukemia virus type I transactivator protein Tax. J Biol Chem 2003;278:21814–21822.
29. Tsuji T, Sheehy N, Gautier VW, Hayakawa H, Sawa H, and Hall WW: The nuclear import of the human T lymphotropic virus type I (HTLV-1) tax protein is carrier- and energy-independent. J Biol Chem 2007;282:13875–13883.
30. Alefantis T, Flaig KE, Wigdahl B, and Jain P: Interaction of HTLV-1 Tax protein with calreticulin: Implications for Tax nuclear export and secretion. Biomed Pharmacother 2007;61:194–200.
31. Avesani F, Romanelli MG, Turci M, *et al.:* Association of HTLV Tax proteins with TAK1-binding protein 2 and RelA in calreticulin-containing cytoplasmic structures participates in Tax-mediated NF-κB activation. Virology 2010; 408:39–48.
32. Ramírez E, Cartier L, and Flores R: In vitro cytoskeleton changes of mouse neurons induced by purified HTLV-1, and PBMC from HAM/TSP patients and HTLV-1 carriers. Arch Virol 2004;149:2307–2317.
33. Hanon E, Hall S, Taylor GP, *et al.:* Abundant tax protein expression in CD4+ T cells infected with human T-cell lymphotropic virus type I (HTLV-1) is prevented by cytotoxic T lymphocytes. Blood 2000;95:1386–1392.
34. Miwa M, Shimotohno K, Hoshino H, Fujino M, and Sugimura T: Detection of pX proteins in human T-cell leukemia virus (HTLV)-infected cells by using antibody against peptide deduced from sequences of X-IV DNA of HTLV-1 and Xc DNA of HTLV-1I proviruses. Gann 1984; 75:752–755.
35. Takeuchi K, Kobayashi N, Nam SH, Yamamoto N, and Hatanaka M: Molecular cloning of cDNA encoding gp68 of adult T-cell leukaemia-associated antigen: Evidence for expression of the pX IV region of human T-cell leukaemia virus. J Gen Virol 1985;66:1825–1829.
36. Journo C, Douceron E, and Mahieux R: HTLV-1 gene regulation: Because size matters, transcription is not enough. Future Microbiol 2009;4:425–440.
37. Nejmeddine M, Barnard A, Tanaka Y, Taylor G, and Bangham C: Human T lymphotropic virus type 1, Tax protein triggers microtubule reorientation in the virological synapse. J Biol Chem 2005;280:29653–29660.
38. Irish BP, Khan ZK, Jain P, *et al.:* Molecular mechanisms of neurodegenerative diseases induced by human retroviruses: A review. Am J Infect Dis 2009;5:231–258.
39. Lepoutre V, Jain P, Quann K, Wigdahl B, and Khan KK: Role of resident CNS cell populations in HTLV-1-associated

neuroinflammatory disease. Front Biosci 2009;14: 1152–1168.
40. Xiao G: NF-kappaB activation: Tax sumoylation is out, but what about Tax ubiquitination? Retrovirology 2012;9:78.
41. Gold LI, Eggleton P, Sweetwyne MT, *et al.:* Calreticulin: non-endoplasmic reticulum functions in physiology and disease. FASEB J 2010;24:665–683.
42. Wang WA, Groenendyk J, and Michalak M: Calreticulin signaling in health and disease. Int J Biochem Cell Biol 2012;44:842–846.
43. Ferreira V, Molina MC, Schwaeble W, Lemus D, and Ferreira A: Does Trypanosoma cruzi calreticulin modulate the complement system and angiogenesis? Trends Parasitol 2005;21:169–174.
44. Li HC, Fujiyoshi T, Lou H, *et al.:* The presence of ancient human T-cell lymphotropic virus type I provirus DNA in an Andean mummy. Nat Med 1999;5:1428–1432.
45. Gallo RC: Human retroviruses after 20 years: A perspective from the past and prospects for their future control. Immunol Rev 2002;185:236–265.
46. Sugamura K, Fujii M, Ueda S, and Hinuma Y: Identification of a glycoprotein, gp21, of adult T cell leukemia virus by monoclonal antibody. J Immunol 1984;132:3180–3184.
47. Michalak M, Corbett EF, Mesaeli N, Nakamura K, and Opas M: Calreticulin: One protein, one gene, many functions. Biochem J 1999;344(Pt 2):281–292.
48. Yasunaga J, Lin FC, Lu X, and Jeang KT: Ubiquitin-specific peptidase 20 targets TRAF6 and human T cell leukemia virus type 1 tax to negatively regulate NF-kappaB signaling. J Virol 2011;85:6212–6219.
49. Shembade N, Harhaj NS, Yamamoto M, Akira S, and Harhaj EW: The human T-cell leukemia virus type 1 Tax oncoprotein requires the ubiquitin-conjugating enzyme Ubc13 for NF-kappaB activation. J Virol 2007;81:13735–13742.

Address correspondence to:
Maria Antonieta Valenzuela
Departamento de Bioquímica y Biología Molecular
Facultad de Ciencias Químicas y Farmacéuticas
Universidad de Chile
Sergio Livingstone 1007
Santiago 233
Chile

E-mail: mavalenz@uchile.cl

Vaccine 32 (2014) 864–871

Contents lists available at ScienceDirect

Vaccine

journal homepage: www.elsevier.com/locate/vaccine

Tricomponent fusion complex comprising a viral antigen, a pentameric α-helical coiled-coil, and an immunoglobulin-binding domain as an effective antiviral vaccine

Takeshi Arakawa[a,b,*], Tetsuya Harakuni[a], Takeshi Miyata[a], Senji Tafuku[c], Masayuki Tadano[d]

[a] *Molecular Microbiology Group, Department of Tropical Infectious Diseases, COMB, Tropical Biosphere Research Center, University of the Ryukyus, 1 Senbaru, Nishihara, Okinawa 903-0213, Japan*
[b] *Division of Host Defense and Vaccinology, Department of Microbiology, Graduate School of Medicine, University of the Ryukyus, 207 Uehara, Nishihara, Okinawa 903-0215, Japan*
[c] *Jectas Innovators Co. Ltd., 1 Senbaru, Nishihara, Okinawa 903-0213, Japan*
[d] *Department of Molecular Virology, Graduate School of Medicine, University of the Ryukyus, 207 Uehara, Nishihara, Okinawa 903-0215, Japan*

ARTICLE INFO

Article history:
Received 26 August 2013
Received in revised form 5 December 2013
Accepted 10 December 2013
Available online 24 December 2013

Keywords:
Japanese encephalitis virus E protein
α-Helical coiled-coil
Cartilage oligomeric matrix protein
Delivery system
Vaccine

ABSTRACT

The pentameric coiled-coil domain of cartilage oligomeric matrix protein (COMP) genetically fused to the Z domain of *Staphylococcus aureus* protein A, an immunoglobulin-binding domain (IBD), was evaluated as a viral antigen carrier complex. In a proof-of-concept study, recombinant Japanese encephalitis virus (JEV) E protein domain III (D3) was loaded onto the COMP–Z fusion protein by chemical conjugation, and the tricomponent complex generated, COMP–Z/D3, was evaluated for its vaccine efficacy in a mouse JEV infection model. Immunization with the complex conferred substantially greater protection against lethal JEV infection than the unloaded antigen. Next, a tricomponent complex was engineered in which the three molecular entities (the D3 antigen, COMP coiled-coil domain, and Z domain) were genetically connected in tandem to create the D3–COMP–Z tricomponent complex, or its reversal oriented construct, Z–COMP–D3. The fusion complexes were produced as inclusion bodies in *Escherichia coli*, but could be refolded to biologically active pentamers that retained the E protein antigenicity and the IBD function. Immunization with the refolded complexes conferred a high level of protection against lethal JEV infection, similar in efficacy to that of the tricomponent complex generated by chemical conjugation. These results demonstrate that the tricomponent complex, whether generated by chemical or genetic fusion, is a promising molecular design for the creation of effective subunit vaccines against viral infections.
© 2014 Elsevier Ltd. All rights reserved.

1. Introduction

Innocuous protein antigens can become effective vaccines against infectious diseases if their immunogenicity is strongly augmented. For this reason, their coadministration with adjuvants, which induce innate immunity, is the most practical approach to eliciting the adaptive immunity represented by antibody and/or cell-mediated immune responses. Although oil-based adjuvants are promising, they often induce unacceptable reactogenicity, which may lead to the discontinuation of vaccine development. Therefore, the use of moderately strong adjuvants with robust safety, such as those based on aluminum salts (alum), combined with recombinant protein engineering techniques may be a desirable alternative strategy for vaccine design. Specific delivery of antigens to professional antigen-presenting cells (APCs) is one such promising technique [1–3], and when combined with alum adjuvants, may induce a sufficiently strong immune response to effectively control infections.

We recently reported novel antigen delivery molecules that were shown to target B lymphocytes and to robustly augment the immunogenicity of loaded recombinant protein antigens [4]. The delivery system exploits three physically linked molecular entities: (1) a recombinant protein antigen; (2) an APC-targeting ligand; and (3) a multimer-forming antigen scaffold. In our previous study, we created a prototype molecule in which the α-helical coiled-coil domain of cartilage oligomeric matrix protein (COMP) [5] was genetically linked to the Z domain [6], a derivative of the D domain of *Staphylococcus aureus* protein A [4]. The fusion gene was expressed extracellularly by *Escherichia coli* as a pentamer, onto which vaccine candidate antigens of the malarial parasite were

* Corresponding author at: Molecular Microbiology Group, Tropical Biosphere Research Center, COMB, University of the Ryukyus, 1 Senbaru, Nishihara, Okinawa 903-0213, Japan. Tel.: +81 98 895 8974; fax: +81 98 895 8974.
E-mail address: tarakawa@comb.u-ryukyu.ac.jp (T. Arakawa).

0264-410X/$ – see front matter © 2014 Elsevier Ltd. All rights reserved.
http://dx.doi.org/10.1016/j.vaccine.2013.12.016